



# AMERICAN METEOROLOGICAL SOCIETY

*Journal of Hydrometeorology*

## **EARLY ONLINE RELEASE**

This is a preliminary PDF of the author-produced manuscript that has been peer-reviewed and accepted for publication. Since it is being posted so soon after acceptance, it has not yet been copyedited, formatted, or processed by AMS Publications. This preliminary version of the manuscript may be downloaded, distributed, and cited, but please be aware that there will be visual differences and possibly some content differences between this version and the final published version.

The DOI for this manuscript is doi: 10.1175/JHM-D-13-083.1

The final published version of this manuscript will replace the preliminary version at the above DOI once it is available.

If you would like to cite this EOR in a separate work, please use the following full citation:

Elsner, M., S. Gangopadhyay, T. Pruitt, L. Brekke, N. Mizukami, and M. Clark, 2014: How does the Choice of Distributed Meteorological Data Affect Hydrologic Model Calibration and Streamflow Simulations? *J. Hydrometeor.* doi:10.1175/JHM-D-13-083.1, in press.



# How does the Choice of Distributed Meteorological Data Affect Hydrologic Model Calibration and Streamflow Simulations?

Marketa M. Elsner<sup>1</sup>  
Technical Service Center, US Bureau of Reclamation, Denver, CO

Subhrendu Gangopadhyay  
Technical Service Center, US Bureau of Reclamation, Denver, CO

Tom Pruitt  
Technical Service Center, US Bureau of Reclamation, Denver, CO

Levi Brekke  
Technical Service Center, US Bureau of Reclamation, Denver, CO

Naoki Mizukami  
NCAR Research Applications Laboratory, Boulder, CO

Martyn Clark  
NCAR Research Applications Laboratory, Boulder, CO

---

<sup>1</sup> *Corresponding author address:* Marketa M. Elsner, Technical Service Center, U.S. Bureau of Reclamation, Bldg 67 5<sup>th</sup> Floor West, PO Box 25007 (86-68210), Denver, CO 80225-0007.  
E-mail: [melsner@usbr.gov](mailto:melsner@usbr.gov)

24  
25  
26  
27  
28  
29  
30  
31  
32  
33  
34  
35  
36  
37  
38  
39  
40  
41  
42  
43  
44  
45  
46

## Abstract

Spatially distributed historical meteorological forcings (temperature and precipitation) are commonly incorporated into modeling efforts for long-term natural resources planning. For water management decisions, it is critical to understand the uncertainty associated with the different choices made in hydrologic impact assessments (e.g., choice of hydrologic model, choice of forcing dataset, calibration strategy, etc.). This paper evaluates differences among four commonly used historical meteorological datasets and their impacts on streamflow simulations produced using the Variable Infiltration Capacity (VIC) model. The four meteorological datasets examined here have substantial differences, particularly in minimum and maximum temperatures in high elevation regions such as the Rocky Mountains. The temperature differences among meteorological forcing datasets are generally larger than the differences between calibration and validation periods. Of the four meteorological forcing datasets considered, there are substantial differences in calibrated model parameters and simulations of the water balance. However, no single dataset is superior to the others with respect to VIC simulations of streamflow. Also, optimal calibration parameter values vary across case study watersheds and select meteorological datasets, suggesting that there is enough flexibility in the calibration parameters to compensate for the effects of using select meteorological datasets. Evaluation of runoff sensitivity to changes in climate indicates that the choice of meteorological dataset may be as important in characterizing changes in runoff as climate change, supporting consideration of multiple sources of uncertainty in long-term planning studies.

## 47 1. Introduction

48 Use of sophisticated physical process models informed by statistically or dynamically  
49 downscaled climate change scenarios is increasingly becoming an integral part of long term  
50 natural resources planning. For example, the proposed listing of the North American Wolverine  
51 in 2013 as threatened under the Endangered Species Act (Federal Register, Vol. 78, No. 23)  
52 relied, in part, on work done by McKelvey et al. (2011) to evaluate the impacts of climate change  
53 on this distinct population, which depends heavily on contiguous snowpack. In addition, Wenger  
54 et al. (2011) identified opportunities for mitigation efforts to revive populations of trout species  
55 in the interior western United States based on an analysis of future climate change impacts.  
56 Finally, Bentz et al. (2010) utilized population models driven by projected climate scenarios to  
57 identify regions in North America with a high potential for bark beetle outbreak. For  
58 environmental management decisions highlighted by these studies, as well as water management  
59 decisions, understanding the uncertainty associated with various underlying modeling application  
60 choices is critical.

61 In an assessment of climate change impacts on water resources, modeling application  
62 choices may include historical and projected future climate datasets, model structure, and model  
63 calibration metrics, objective function, and calibration scheme. With respect to choice of  
64 historical meteorological forcings, studies have shown that the dataset choice may cause as much  
65 sensitivity in the resulting water balance as the choice of land surface model (Guo et al. 2006), if  
66 not more (Mo et al. 2012). Hossain and Anagnostou (2005) and Maggioni et al (2012)  
67 investigated the relative impact of model and rainfall forcing errors in hydrologic simulations by  
68 land surface models and found that both together contribute a large amount of the uncertainty in  
69 soil moisture estimates. Precipitation appears to cause the greatest sensitivity in runoff (Materia

70 et al. 2009; Nasonova et al. 2011) and that sensitivity is not consistent across watersheds (Xue et  
71 al. 1991). Precipitation estimates are strongly dependent on the method used to interpolate the  
72 data, particularly in regions in the western United States where climate stations, upon which the  
73 datasets are based, are sparse (Mo et al. 2012). Mizukami et al. (2013) compared model  
74 simulations forced by two meteorological datasets (developed using different methodologies)  
75 and found that differences in shortwave radiation estimates have a large impact on hydrologic  
76 states and fluxes, particularly at higher elevation, influencing snow melt and runoff timing as  
77 well as evapotranspiration.

78 Other studies indicate that model structure may influence hydrologic model simulations.  
79 For example, Bohn et al (2013) found that the Thornton and Running (1999) approach for  
80 deriving meteorological forcings based on precipitation and temperature have inconsistent biases  
81 across large spatial domains. Clark et al. (2008) found that model structure is just as important  
82 as the choice of model parameters. Finally, Vano et al. (2012) found that hydrologic model  
83 structure significantly influences runoff sensitivities to changes in precipitation and temperature  
84 (i.e. imposed changes in climate).

85 Further, other studies suggest that calibration method may also affect hydrologic  
86 modeling results. Streamflow simulations may not be sensitive to calibration approach; however  
87 intermediate states such as potential evapotranspiration may differ substantially (Hay et al.  
88 2000). Also, calibration parameters may not be stationary in time and simulation errors may  
89 increase with the time lag between calibration and simulation periods, as found by Merz et al.  
90 (2011) in their analysis of 273 catchments in Austria. With respect to climate change studies,  
91 Wilby (2005) found that the uncertainty in changes in projected future streamflow due to the  
92 choice of calibration period is similar to the uncertainty due to future greenhouse gas emissions

93 scenarios. Also, Vaze et al. (2010) found that results from a hydrologic model calibrated over an  
94 average or wet climatic period are suitable for climate change impact studies where the  
95 difference between historical and predicted future rainfall is within about 15%.

96 Results from the previously mentioned studies suggest that hydrologic model calibration  
97 may be significantly impacted by choice of meteorological forcing dataset. Numerous  
98 meteorological forcing datasets have been developed over parts of the United States and they  
99 commonly consist of daily precipitation, temperature (minimum and maximum), and wind speed,  
100 at a minimum. Historical datasets are often developed based on interpolated data from National  
101 Weather Service daily cooperative observer (Co-op) stations (corrected for elevation) with  
102 specific needs in mind. For example, historical datasets developed by Maurer et al. (2002) and  
103 Livneh et al. (2013) (spanning 1915-2000 and 1915-2011, respectively) encompass the  
104 continental United States (CONUS) and their methodology focuses on the accuracy of spatial  
105 patterns and variability. The dataset developed by Wood and Lettenmaier (2006) (spanning  
106 1915-2005 over the CONUS) was used as the basis of a west-wide seasonal hydrologic forecast  
107 system, which relied on a stations with real-time observations. Datasets by Hamlet and  
108 Lettenmaier (2005), Elsner et al. (2010), and Littell et al. (2011) (all spanning 1915-2006 and  
109 covering parts of the western United States) were developed with the objective of evaluating  
110 long-term climate trends and evaluating implications of climate change. For hydrologic model  
111 applications such as the Variable Infiltration Capacity (VIC) Model (Liang et al. 1994; Liang et  
112 al. 1996), additional meteorological forcings (i.e. humidity and radiative fluxes) need to be  
113 estimated from the diurnal temperature range and precipitation (e.g. using the approach of  
114 Thornton and Running 1999) or taken from other sources such as reanalysis products.

115           There is an increasing number of historical datasets based on reanalysis products such as  
116 the National Centers for Environmental Prediction, North American Regional Reanalysis  
117 (NARR; Mesinger et al. 2006). For example, the North American Land Data Assimilation  
118 System (NLDAS) Phase 2 (Xia et al. 2012) dataset is primarily derived from NARR data and  
119 this dataset is used by Mizukami et al. (2013) in their analysis of model sensitivities to  
120 meteorological forcings in mountainous terrain. Abatzoglou (2011) developed a 4-km gridded  
121 historical climate dataset based on the NLDAS Phase 2 dataset and the monthly 800 meter  
122 PRISM product (Daly et al. 2008).

123           Although there have been an increasing number of scientific studies exploring  
124 uncertainties associated with hydrologic model application choices, these uncertainties are still  
125 not well understood. Further, natural resource managers are increasingly using datasets and  
126 modeling tools, like those previously described, in long-term planning. Federal natural resource  
127 management and conservation agencies, including among others the Bureau of Reclamation  
128 (Reclamation), U.S. Geological Survey, U.S. Fish and Wildlife Service, U.S. Forest Service,  
129 National Oceanic and Atmospheric Association (NOAA), and Pacific Northwest National  
130 Laboratory, all have mandates for incorporating climate change into long-term planning.  
131 Climate projections originate from GCMs at coarse scale in space and time and are typically  
132 downscaled, either statistically or dynamically using a regional climate model, so that they may  
133 be useful for planning studies (e.g. Wood et al. 2004, Salathe et al. 2007, Christensen and  
134 Lettenmaier 2007, Maurer et al. 2007, among others). Statistically downscaled climate  
135 projections, arguably the type of projections most commonly used in long term planning studies,  
136 rely on historical meteorological datasets as the basis for downscaling. Numerous archives of  
137 statistically downscaled climate projections available for various domains within the western

138 United States utilize different historical datasets. For example, archives of hydro-climate  
139 scenarios developed for the Pacific Northwest (Hamlet et al. 2013), as well as major western  
140 United States river basins (Littell et al. 2011) at 1/16th degree spatial resolution, rely on  
141 historical datasets developed by Elsner et al. (2010) and Littell et al. (2011) as the basis for  
142 downscaling. In another example, Maurer et al (2007) developed an archive of statistically  
143 downscaled hydro-climate scenarios covering the CONUS plus contributing areas of Canada,  
144 which have served as a consistent dataset used by Reclamation in numerous basin studies  
145 pursuant to the SECURE Water Act of 2009 (Public Law 111-11), and rely on the historical  
146 dataset developed by Maurer et al. (2002) at 1/8th degree spatial resolution as its basis.

147 Greater understanding of the implications associated with using a particular historical  
148 dataset is important not only for historical hydrologic studies, but also for characterizing the  
149 uncertainty associated with projected future hydrologic conditions. In summary, this paper seeks  
150 to answer two questions:

- 151 (1) Is there an optimal distributed meteorological forcing dataset to be used in simulating  
152 streamflow through the VIC hydrological model?
- 153 (2) How does the choice of distributed meteorological data affect hydrologic model  
154 calibration and sensitivity analysis, particularly with respect to changes in climate?

155 In the following section, we describe the study approach. The study analysis is organized  
156 in two sections. First, we compare four meteorological forcing datasets commonly used in  
157 natural resource studies. Second, we discuss hydrologic model calibrations, using each of the  
158 four compared datasets, and resulting simulations. We conclude with a discussion of key  
159 findings in the context of various uncertainties in long-term natural resources planning studies.

## 160 2. Approach

### 161 2.1 *Historical Meteorological Forcing Datasets*

162 We compile and compare four spatially distributed meteorological datasets that differ in their use  
163 of station observations, handling of temporal inhomogeneities, spatial extent, spatial resolution,  
164 and temporal coverage. The four historical gridded meteorological datasets were developed by:  
165 1) Maurer et al. (2002) – hereafter called the Maurer dataset; 2) Wood and Lettenmaier (2006) –  
166 hereafter called the Wood-Lettenmaier dataset; 3) Abatzoglou (2011) – hereafter called the  
167 Abatzoglou dataset; and 4) Elsner et al. (2010), expanded by Littell et al. (2011) – hereafter  
168 called the Elsner-Littell dataset (datasets are summarized in Table 1). We compare precipitation  
169 and temperature (maximum, minimum, and diurnal range) from these datasets over a common  
170 time period (water years 1980-1999), spatial resolution (1/8 degree), and domain, generally the  
171 United States portions of four major western hydrologic regions, including the Pacific Northwest  
172 (Columbia River Basin plus coastal drainages in Oregon and Washington); California; the Great  
173 Basin; the Colorado River Basin; and, the Missouri River basin west of 93 degrees west  
174 longitude (Fig. 1). The Maurer and Wood-Lettenmaier datasets have a native spatial resolution  
175 of 1/8 degree and use a common grid, consistent with the North American Land Data  
176 Assimilation System (NLDAS, Mitchell et al. 2004). The Abatzoglou and Elsner-Littell datasets  
177 were aggregated from their native resolution (4-km and 1/16th degree, respectively) to the same  
178 common 1/8 degree grid, using a local area averaging approach. Consequences of aggregating  
179 precipitation and temperature from these datasets are not explored in this study. However, we  
180 may speculate reduced error in precipitation and temperature aggregated from finer scale to 1/8  
181 degree due to the fact that coarse station observations are the basis for development of both  
182 Abatzoglou and Elsner-Littell datasets. In addition, Gangopadhyay et al. (2004) evaluated the

183 impacts of spatial aggregation on precipitation forecast skill in the context of statistically  
184 downscaled precipitation estimates. They found that spatial averaging either had little effect or  
185 increased the skill of downscaled precipitation estimates. Additional studies may be needed to  
186 evaluate the issue of scale of meteorological data for watersheds smaller than those considered in  
187 this study (the smallest of which is 1,792 square kilometers). Distinguishing characteristics of  
188 the four datasets are summarized in Table 1. We refer to their associated publications for details  
189 regarding the purpose and applications of each dataset, and the approaches taken in developing  
190 them.

191         The Maurer, Wood-Lettenmaier, and Elsner-Littell gridded precipitation fields are  
192 primarily based on the Co-op Station Network (along with similar networks in Canada and  
193 Mexico), interpolated to a grid using the SYMAP algorithm (Shepard 1984). The Maurer dataset  
194 only includes stations with more than 20 years of data from 1949-2000. The Wood-Lettenmaier  
195 dataset only includes stations that have both long term records and report in real time (through  
196 2005). These stations have at least 45 years of record and at least 80% coverage of the period  
197 between 1915 and 2005 (Wood 2008). The Elsner-Littell dataset follows the approach of Hamlet  
198 and Lettenmaier (2005) and only includes stations with at least 5 years of data and at least one  
199 continuous year from 1915-2006. The dataset is then corrected for temporal inhomogeneities by  
200 use of monthly Historical Climatology Network (HCN) data (and Canadian equivalent).

201 Precipitation fields from all three of the above mentioned datasets incorporate a correction to  
202 monthly climatologies from the Parameter-elevation Regressions on Independent Slopes Model  
203 (PRISM) (Daly et al. 2008) albeit for slightly different time periods (1961-1990 for Maurer and  
204 Wood-Lettenmaier datasets and 1971-2000 for Elsner-Littell dataset). The Abatzoglou  
205 precipitation fields are derived from NLDAS Phase 2 data (Xia et al. 2012), comprised of gage

206 data (Co-op stations included), radar, and reanalysis data (at 32-km spatial resolution). The  
207 Abatzoglou dataset applies a secondary correction to the monthly 800 meter PRISM timeseries.

208         Temperature (minimum and maximum) fields in the Maurer, Wood-Lettenmaier, and  
209 Elsner-Littell datasets are also obtained from Co-op stations (station mix as described for  
210 precipitation) and are lapsed (at -6.5 degrees Celsius [C] per km) to the mean grid cell elevation.  
211 The Elsner-Littell dataset, however, applies a secondary correction of average temperature to the  
212 PRISM climatologies (preserving the range between minimum and maximum temperature in Co-  
213 op station data). The Abatzoglou temperature fields are based on NLDAS Phase 2 and a  
214 secondary correction to monthly 800 meter PRISM timeseries.

215         The Maurer, Wood-Lettenmaier, and Elsner-Littell datasets rely on wind speeds from  
216 NLDAS Phase 1, which are downscaled wind fields from the National Centers for  
217 Environmental Prediction – National Center for Atmospheric Research (NCEP-NCAR)  
218 reanalysis products (Kalanay et al. 1996). The wind speeds in the Abatzoglou dataset are taken  
219 from the NLDAS Phase 2, which is based on the NCEP North American Regional Reanalysis  
220 (NARR). Barsugli et al. (2012) found that, in Colorado, NARR windspeeds are substantially  
221 greater than NCEP-NCAR windspeeds at higher elevations and that NARR windspeeds more  
222 closely compare with available observations. They also demonstrate that choice of windspeed  
223 data may impact resulting streamflow simulations. However, we choose not to compare  
224 differences in wind speed in this study, in part because there is less confidence overall in gridded  
225 windspeed data, and the use of the Abatzoglou dataset with NARR windspeeds helps to  
226 demonstrate the sensitivity of simulated streamflow to changes in meteorological forcings.

## 227 2.2 *Case Study Watersheds*

228 We investigate the implications of model calibration using each of these datasets on seven case  
229 study watersheds across the domain, namely: 1) Animas River at Durango, CO (USGS ID  
230 09361500, hereafter called ANIMS); 2) Dolores River near Cisco, UT (USGS ID 09180000,  
231 hereafter called DOLOR); 3) Green River at Green River, UT (USGS ID 09315000, hereafter  
232 called GREEN); 4) Missouri River at Toston, MT (USGS ID 06054500, hereafter called  
233 MISSO); 5) Sacramento River at Bend Bridge near Red Bluff, CA (USGS ID 11377200,  
234 hereafter called SACRB); 6) Salt River near Chrysotile, AZ (USGS ID 09497500, hereafter  
235 called SALTC); and, 7) Snake River near Heise, ID (USGS ID 13037500, hereafter called  
236 SNAKE).

237 Specifically, we explore whether calibration of a hydrologic model using one  
238 meteorological dataset yields significantly different calibration parameters than a model  
239 calibrated using a different meteorological dataset. Further, we explore whether a hydrologic  
240 model calibrated to one meteorological dataset yields significantly different results when forced  
241 with a different meteorological dataset. Lastly, we explore the sensitivity of runoff to changes in  
242 climate (as represented by differences between calibration and validation periods) using the four  
243 calibrated models. Direct comparisons of the distributed meteorological datasets and evaluation  
244 of hydrologic model simulations over the case study watersheds allows us to better understand  
245 the implications of these datasets with respect to long-term planning studies.

## 246 2.3 *Modeling Scheme*

247 To represent physical hydrologic processes in the seven case study watersheds, we apply the VIC  
248 hydrologic model. The VIC model has been widely used in large scale hydrologic studies across  
249 the globe and to explore the implications of climate change on water and other resources

250 including forests, agriculture, fish and wildlife (e.g. Christensen and Lettenmaier 2007, Elsner et  
251 al. 2010, Wenger et al. 2011). It was employed in the same studies for which three of the four  
252 comparison datasets were developed, with the exception of the Abatzoglou dataset. The VIC  
253 model was also used to validate the datasets developed as part of the NLDAS project (Mitchell et  
254 al. 2004, Xia et al. 2012). The model configuration used here is consistent with that used in the  
255 Reclamation's West-wide Climate Risk Assessment (Reclamation 2011). Namely, we apply VIC  
256 model version 4.0.7 (also used by Elsner et al. 2010 and Hamlet et al. 2013) to simulate surface  
257 runoff and baseflow per model grid cell. We then apply the Lohmann et al. (1998) model to  
258 route surface runoff and baseflow to select locations, producing simulated natural streamflow.  
259 Natural flows are defined as streamflow that would exist in the absence of diversions and return  
260 flows resulting from human activities. Hydrologic model simulations are performed in water  
261 balance mode using a daily time step water balance and 1-hour time step internal snow model.

262       VIC model calibration is conducted using the multi-objective complex evolution  
263 approach developed by Yapo et al. (1998). The user may define the calibration parameters, and  
264 the objectives (calibration metrics) on which to base the objective function. Pareto sets are  
265 theoretically equal in terms of their objective functions. As such, one set of parameters was  
266 generally chosen manually from the Pareto optimal set. Bennett et al. (2012) showed that the  
267 choice of model parameter set within the Pareto optimal set had minimal impact on resulting  
268 hydrologic simulations in analyzed watersheds of British Columbia. Calibrations are repeated up  
269 to seven times to ensure parameters were globally optimal and to account for lack of  
270 convergence in some calibrations. Calibration metrics include three error statistics computed  
271 between simulated and reconstructed natural streamflow, which is considered the best estimate  
272 of observed natural conditions. The objective function for calibration is computed based on

273 three metrics: the Nash-Sutcliffe Efficiency computed using monthly flows ( $NSE_{mon}$ ), the root  
274 mean squared error of monthly flows divided by the observed mean monthly flow ( $RMSE_{mon}$ ),  
275 and the normalized error in mean monthly flow volume ( $VolErr_{mon}$ ). These metrics were chosen  
276 to reduce errors in seasonal timing and magnitude of flow ( $NSE_{mon}$  and  $RMSE_{mon}$ ) as well as  
277 reduce error in annual flow volume ( $VolErr_{mon}$ ). All three metrics generally have values between  
278 0 and 1; however,  $VolErr_{mon}$  is generally quite low, effectively giving the  $NSE_{mon}$  and  $RMSE_{mon}$   
279 metrics relatively greater weight. The  $NSE_{mon}$  function emphasizes the high-peak flow periods  
280 and therefore produces parameters that optimize hydrograph performance during the seasonal  
281 peak (Bennett et al. 2012, Clark et al. 2008). The  $VolErr_{mon}$  strictly emphasizes volume  
282 conservation over the calibration period and is not responsive to errors in streamflow timing or  
283 seasonality (Bennett et al. 2012).

284 We evaluate the sensitivity of streamflow to variations in common VIC model calibration  
285 parameters over the seven case study watersheds in order to determine the most appropriate  
286 calibration parameter set. Model parameters considered for calibration are summarized in Table  
287 2. Sensitivity is evaluated based on perturbation experiments spanning the accepted range of  
288 each parameter. The three calibration metrics described above are computed for each  
289 perturbation experiment and metrics are compared across case study watersheds. Parameter  
290 sensitivity may be dependent on watershed, making it difficult to apply a stringent threshold for  
291 each calibration watershed. Therefore, for a single parameter, if the majority (i.e. more than  
292 half) of the metrics for all calibration watersheds varies by less than 10 percent, that parameter is  
293 considered insensitive. Based on this sensitivity analysis, the following parameters were chosen:  
294  $D_s$ ,  $W_s$ ,  $D_{smax}$ ,  $D_2$ , and  $D_3$ .  $D_s$ ,  $W_s$ , and  $D_{smax}$  are parameters that define the shape of the  
295 baseflow curve (Liang et al. 1994).  $D_2$  and  $D_3$  consist of the depth of the middle and deepest of

296 three model soil layers. Other parameters, including the parameter defining the shape of the  
297 variable infiltration capacity curve (bi), wind speed attenuation through the canopy, snow  
298 roughness, radiation attenuation in the canopy, and routing flow velocity, were found to  
299 minimally contribute to VIC model sensitivity and were not modified during calibration (Table  
300 2). Choosing appropriate calibration parameters, while limiting the number, allows for  
301 successful and more computationally efficient model calibrations (Kampf and Burges 2007).

#### 302 2.4 *Evaluation Methods*

303 Model simulations are performed over seven case study watersheds to evaluate the implications  
304 of using different meteorological datasets on simulated streamflow. Case study watersheds  
305 represent each of the major western United States watersheds under Reclamation's purview and  
306 vary in size, elevation, aspect, and climatic conditions. The time period of model calibration and  
307 validation is dictated by the length of record of available observed reconstructed natural  
308 streamflow and meteorological data, but is also chosen to include a range of hydrologic  
309 conditions. Table 3 summarizes the characteristics of each case study watershed and identifies  
310 their model calibration/validation periods.

311 To evaluate the implications of VIC model calibration on simulated streamflow, we  
312 employ a procedure where the VIC model is calibrated for each of the case study watersheds and  
313 using one of the four select meteorological datasets. Each calibrated model is then forced with  
314 the remaining three meteorological datasets. Resulting simulated mean monthly hydrographs for  
315 each watershed are compared with reconstructed natural streamflow.

316 The sensitivity of runoff to changes in climate is also explored using the calibrated  
317 simulations by partitioning the validation period for each case study watershed (generally a 10  
318 year period, but 5 years for MISSO and 7 years for ANIMS; see Table 3) into cool-wet and

319 warm-dry water years. Cool-wet and warm-dry validation years were selected based on their  
320 computed difference (in percent and degrees C, respectively) from the median of annual  
321 precipitation and temperature over the simulation period, 1980-1999 water years. Since the  
322 change in climate between calibration and validation periods for most case study watersheds  
323 (except MISSO) is as great as the change in climate between meteorological datasets, we choose  
324 these two converse year types to help demonstrate the greatest potential change in runoff  
325 sensitivity due to dataset choice and provide context for potential implications. Unique groups  
326 of years were selected and averaged to generate mean annual precipitation, temperature, and  
327 runoff for each case study watershed and meteorological forcing dataset. However, some years  
328 were commonly classified as cool-wet and warm-dry for most watersheds and meteorological  
329 forcing datasets (e.g. water year 1982 was a common cool-wet year, while 1981 was a common  
330 warm-dry year). For each calibrated model, change in mean annual runoff between calibration  
331 period and each of the two validation year types (as a function of change in climate - mean  
332 annual precipitation and temperature) is computed to determine whether runoff sensitivity  
333 changes with change in climate or meteorological forcing dataset.

### 334 3. Comparison of Spatially Distributed Meteorological Data

335 Four meteorological forcing datasets (Maurer, Wood – Lettenmaier, Abatzoglou, and Elsner –  
336 Littell) are compared across a common study domain (see purple dashed line in Fig. 1) and time  
337 period (1980-1999 water years). The datasets are compared with respect to precipitation (Prcp)  
338 and temperature (minimum [Tmin], maximum [Tmax], and diurnal range [Tran]). Across the  
339 common domain, datasets are compared based on their means, standard deviation, and  
340 correlations. Similar analyses are performed over a longer period (1950-1999 water years), with  
341 the exception of the Abatzoglou dataset (which begins in 1979), and comparable results are

342 found and, therefore, not presented. In addition to a comparison across the study domain, the  
343 datasets are compared over seven case study watersheds based on monthly values over  
344 calibration, validation, and simulation periods. For both sets of comparisons, statistics are  
345 computed using monthly and annual totals for precipitation and daily averages over the month or  
346 year for temperature.

### 347 *3.1 Differences in Meteorological Forcings across Study Domain*

348 Figures 2 through 7 illustrate monthly and annual statistics for all four variables. Values are  
349 presented as comparisons of the Abatzoglou (A), Elsner-Littell (EL), and Wood-Lettenmaier  
350 (WL) datasets to the Maurer (M) dataset. The Maurer dataset is commonly used in statistical  
351 downscaling efforts and is the baseline historical dataset used in Reclamation's West Wide  
352 Climate Risk Assessment (Reclamation 2011). It is therefore used as the basis for comparison of  
353 the remaining three datasets. Figures 2 and 3 show percent differences in precipitation statistics  
354 between datasets (computed over 1980-1999 water years), while Figures 4 through 7 show  
355 absolute differences in temperature statistics in degrees C. Boxplots in Figures 2 and 4 through 6  
356 compare annual values across VIC grid cells, where the boxes represent the 25th, 50th, and 75th  
357 percentile values, while the whiskers represent the 5th and 95th percentiles. Monthly statistics  
358 were similarly analyzed, but the results are not presented here, as they are consistent with annual  
359 statistics overall. However, notable differences between monthly and annual statistics are  
360 discussed. Figures 3 and 7 illustrate how precipitation and temperature (Tmax, Tmin, and Tran)  
361 vary spatially in winter and summer, represented by January and July, respectively.

362 Results show considerable differences in precipitation among datasets, both in terms of  
363 distribution of statistics (Fig 2) and spatial differences (Fig. 3). In particular, note that over 50%  
364 of grid cells in Fig. 2 have differences in precipitation greater than 10%, as can be seen by the

365 difference between 25<sup>th</sup> and 75<sup>th</sup> percentile values. Although there are considerable differences  
366 in some parts of the domain (Fig. 3), the medians of precipitation difference are close to zero (5  
367 percent or less). Monthly analysis shows greater a distribution of differences in July than other  
368 months, likely corresponding with a smaller magnitude of precipitation occurring in much of the  
369 western United States in summer. In January, the Maurer dataset generally has more  
370 precipitation (median negative difference on the order of 5-10 percent) in the northern portion of  
371 the domain (defined as north of the California-Oregon border at 42 degrees N latitude) and less  
372 precipitation (median positive difference on the order of 0-5 percent) in the southern portion of  
373 the domain, compared with the alternate datasets (Fig. 3). In July, the Maurer dataset generally  
374 has less precipitation than the compared datasets in all regions. The exceptions include a median  
375 negative difference in California of about 38 percent comparing it with the Wood-Lettenmaier  
376 dataset, and of about 4 percent comparing it with the Elsner-Littell dataset. To put these results  
377 in context, consider that many future climate projections suggest changes in precipitation within  
378 +/- 10% by the 2050s (Reclamation 2011). The differences are notable, despite the expectation  
379 that the Wood-Lettenmaier dataset is more similar to the Maurer dataset with respect to  
380 precipitation, than either the Elsner-Littell or Abatzoglou dataset, due to the use of the same  
381 PRISM dataset for secondary corrections, namely the 1961-1990 climatology. PRISM  
382 climatologies cannot be directly compared and, by extension, cannot be attributed as the sole  
383 source of differences between datasets because their products incorporate data improvements and  
384 station networks and underlying data are not consistent between products.

385         There are also considerable differences in temperature among datasets (Fig. 4 showing  
386 mean annual maximum temperature, Fig. 5 showing mean annual minimum temperature, Fig. 6  
387 showing mean annual diurnal temperature range, and Fig. 7 showing spatial differences for

388 January and July). Specifically, the Elsner-Littell dataset shows differences in mean annual  
389 maximum temperature greater than 1 degree C for approximately 25% of grid cells (Fig.), while  
390 Elsner-Littell and Abatzoglou datasets show differences in mean annual minimum temperature  
391 greater than 1 degree C for approximately 25% of grid cells (Fig. 4), with the Abatzoglou dataset  
392 showing minimum temperature differences in the daily mean greater than 2 degrees C for  
393 approximately 25% of grid cells. Monthly analysis shows the greatest distribution of differences  
394 occurs in the cool season (approximately September to March). Temperature differences are  
395 most pronounced in high elevation areas, especially throughout the Rocky Mountains (Fig. 7).  
396 Additionally, the Abatzoglou dataset has a generally lower diurnal temperature range than the  
397 Maurer dataset, particularly during July. As described in section 2.1, the datasets differ in their  
398 corrections of temperature by elevation. Maurer and Wood-Lettenmaier datasets impose a  
399 constant lapse rate (-6.5 degrees C per km) in the gridding of temperature from station  
400 observations, while the Abatzoglou and Elsner-Littell datasets incorporate corrections to finer  
401 scale PRISM temperature climatologies (described in section 2.1), causing substantial  
402 differences in daily mean minimum and maximum temperatures, particularly at higher  
403 elevations. A lapse rate of -6.5 degrees C per km appears to be too high for temperature based  
404 on recommended lapse rates in complex terrain (e.g. Blandford et al. 2008; Minder et al. 2010).  
405 Blandford et al. (2008) found that this lapse rate may be applicable to maximum temperature, but  
406 grossly overestimates actual lapse rates for daily minimum and mean temperature. Mizukami et  
407 al. (2013) further discuss the significant implications of the use of a constant lapse rate on the  
408 diurnal temperature range and empirical estimates of shortwave radiation.

409 In comparison of standard deviation between three datasets (Abatzoglou, Elsner-Littell,  
410 Wood-Lettenmaier) to the Maurer dataset, it is evident that the Wood-Lettenmaier dataset has

411 more similar variability than the other datasets for Prcp (Fig. 2). However for temperature,  
412 (Tmin, Tmax, and Tran) the variability is generally comparable (see Figs. 4 through 6).  
413 Correlation between datasets across the entire study domain is highest between Abatzoglou and  
414 Maurer datasets for precipitation and temperature (Tmin, Tmax, and Tran) and generally lowest  
415 between Elsner-Littell and Maurer datasets, which is interesting provided Abatzoglou and  
416 Elsner-Littell datasets both apply temperature corrections based on PRISM climatologies. It may  
417 be speculated that for the Elsner-Littell dataset, the use of monthly HCN (and Canadian  
418 equivalent) station data to correct for temporal inhomogeneities in precipitation and temperature,  
419 due to the use of relatively short station records (minimum of 5 years, with one year of  
420 continuous data), may alter daily precipitation values enough to cause the lower correlations  
421 between the Elsner-Littell and Maurer datasets for precipitation and temperature (and generally  
422 lower correlations between Elsner-Littell and other datasets as well, although results are not  
423 shown). The Abatzoglou dataset, which is based on a combination of CPC daily gage data and  
424 National Weather Service Stage II radar, does not incorporate a similar monthly correction factor  
425 using HCN station data.

### 426 *3.2 Differences in Meteorological Forcings across Basins*

427 Figure 8 summarizes differences in mean annual precipitation and temperature (average [Tavg],  
428 Tmax, and Tmin) between Abatzoglou, Elsner-Littell, Wood-Lettenmaier and the reference  
429 Maurer dataset. These differences are shown for calibration, validation, and overall simulation  
430 periods, and over the seven case study watersheds, which span a range of geographic regions and  
431 elevations. The figure informs analysis of hydrologic model calibration and simulations (section  
432 4). Case study watersheds are presented in order of mean watershed elevation; the watershed

433 with the lowest mean elevation (SACRB) is on the far left of each figure panel, while the  
434 watershed with the highest mean elevation (ANIMS) is on the far right.

435 Calibration and validation periods (as well as overall simulation period which includes  
436 both) for each case study watershed are generally similar in climate, with precipitation  
437 differences generally less than 10% and temperature differences less than 0.5 degrees C. The  
438 MISSO watershed is the exception, where mean annual precipitation over the calibration and  
439 validation periods differ by 18-20%.

440 Interestingly, substantial differences are evident between alternate meteorological forcing  
441 datasets and the Maurer reference dataset. Figure 8 shows that for temperature, the differences  
442 among datasets are larger than the differences between calibration and validation periods, with  
443 differences up to 3 degrees C. For precipitation, the differences among meteorological forcing  
444 datasets are comparable with differences between calibration and validation periods, with  
445 differences generally less than 10% with the exception of the MISSO basin (as previously  
446 described).

447 Specifically, Abatzoglou and Elsner-Littell datasets have higher daily average  
448 temperature than Maurer and Wood-Lettenmaier datasets for all case study watersheds, with the  
449 differences in daily average temperature are primarily driven by differences in the daily  
450 minimum for the Abatzoglou dataset and daily maximum for the Elsner-Littell dataset. Mean  
451 annual precipitation between the four meteorological forcing datasets is within +/- 10% in each  
452 of the case study watersheds. Higher elevation watersheds (SNAKE and ANIMS watersheds)  
453 exhibit the greatest difference in temperature between these datasets for reasons described in  
454 section 3.

## 455 4. Hydrologic Model Simulations for Case Study Watersheds

456 Hydrologic model calibrations and simulations for seven case study watersheds are evaluated to  
457 improve our understanding of potential impacts of meteorological forcings on model calibration  
458 parameters.

### 459 *4.1 Differences in Calibrated Parameters and Model Performance*

460 Each of the seven case study watersheds is calibrated through implementation of an automated  
461 multiple objective approach using the VIC hydrologic model. Table 4 summarizes the resulting  
462 optimal parameter values. In general, there does not appear to be a relationship between optimal  
463 parameters and either watershed or meteorological dataset. This suggests that different  
464 parameter combinations may result in similar objective function values for a given watershed  
465 and meteorological forcing dataset. Alternatively, it may suggest that optimal parameter  
466 combinations may not coincide with the best representations of model physics, but instead are  
467 compensating for biases in forcing data and weaknesses in model structure.

468 Model performance during calibration and validation periods does not depend on the  
469 choice of meteorological dataset (Table 5). The  $NSE_{mon}$ , which is used as a hydrologic metric to  
470 evaluate model simulations of seasonal flow volume and timing and the characteristic shape of  
471 the hydrograph, is above 0.70 for all but one model calibration (MISSO watershed calibrated  
472 using the Elsner-Littell dataset), indicating a good fit between simulated and reconstructed  
473 natural streamflow ( $NSE_{mon}$  may vary between  $-\infty$  and 1, with 1 being perfect). Calibration of  
474 SNAKE and SACRB watersheds result in the highest  $NSE_{mon}$  (between 0.93 and 0.98 for  
475 SNAKE and between 0.92 and 0.95 for SACRB), consistently across models calibrated with  
476 each meteorological dataset. Calibration of DOLOR and MISSO result in the lowest  $NSE_{mon}$

477 values, but still close to or above 0.70 (between 0.76 and 0.78 for DOLOR and between 0.69 and  
478 0.80 for MISSO). Similar results are evident for  $RMSE_{mon}$ . There is not one meteorological  
479 dataset that results in model calibrations with more optimal (higher)  $NSE_{mon}$  values, indicating  
480 that the quality of the datasets are comparable or there is enough flexibility in the model  
481 parameters to compensate for differences among forcing datasets.

#### 482 *4.2 Assessment of Compensatory Errors*

483 We evaluate the forcing of calibrated models for the case study watersheds (to each of the four  
484 meteorological forcing datasets) with alternate forcing datasets (Fig. 9) to understand the  
485 influence of meteorological datasets on streamflow, as well as of the sensitivity of model  
486 simulations to calibration. In Fig. 9, the meteorological dataset listed in the legend title for each  
487 panel is the “base” meteorological dataset used for model calibration. The red solid line in each  
488 panel illustrates the resulting mean monthly hydrograph from “base” calibrated simulations,  
489 having corresponding dataset and calibration parameters. The colored dashed lines illustrate  
490 mean monthly hydrographs from simulations using the calibrated parameters from the base  
491 simulation along with alternate meteorological datasets. The solid black line in each panel  
492 illustrates the mean monthly reconstructed natural streamflow hydrograph.

493 For the ANIMS watershed, simulated flow resulting from models calibrated with  
494 Abatzoglou and Wood-Lettenmaier datasets (second and fourth panels from left) are closer to  
495 reconstructed natural streamflow than flow resulting from models calibrated with the other  
496 datasets (see calibration statistics in Table 5). Also, models calibrated with Elsner-Littell and  
497 Maurer datasets (first and third panels from left), when forced with the Abatzoglou dataset,  
498 perform better than the calibrated models themselves (e.g.  $NSE_{mon}$  improved from 0.70 to 0.81 in  
499 the Elsner-Littell calibrated model and from 0.84 to 0.87 in the Maurer calibrated model).

500 However, in each of the simulations, model calibration and meteorological dataset combination  
501 do little to change the magnitude of flows during the low flow period (autumn and winter).

502 For the DOLOR watershed, forcing calibrated models using alternate meteorological  
503 datasets does not improve existing errors in the calibrated models in flow magnitude during  
504 autumn and winter months. The model calibrated using the Wood-Lettenmaier meteorological  
505 dataset (fourth panel from left) more closely captures the mean reconstructed natural streamflow  
506 seasonal peak magnitude and has the best calibration error statistics of the four calibrated  
507 DOLOR models.

508 For the GREEN watershed, each of the calibrated models results in mean monthly  
509 hydrographs that closely correspond with reconstructed natural streamflow and the forcing of  
510 these models with alternate datasets does not significantly change the results. It may be  
511 speculated that the relative insensitivity of simulated streamflow to forcing dataset or calibration  
512 parameters in the GREEN watershed is likely due the relatively large size of the GREEN  
513 watershed compared with other case study watersheds as well as its hydrologic characteristics.  
514 The GREEN watershed (approximately 116,000 square kilometers) is approximately three times  
515 larger than the next largest case study watershed, MISSO (approximately 40,000 square  
516 kilometers). Compensatory errors have a greater tendency to negate each other in a larger  
517 watershed, resulting in simulations that closely correspond with reconstructed natural flow. For  
518 example, errors in interpolated meteorological station data are more likely to impact a small  
519 watershed that may have few or no stations within it. Also, GREEN is a snowmelt dominant  
520 watershed, which reduces the relative effects of other processes on the water balance (such as  
521 effects of subsurface flow).

522 For the MISSO watershed, each of the calibrated models results in mean monthly  
523 hydrographs that do not correspond well with reconstructed natural streamflow with respect to  
524 the seasonal peak. It appears that over this watershed the Elsner-Littell and Abatzoglou datasets  
525 yield similar flows because, in the left most panel (model calibrated with Elsner-Littell dataset),  
526 the simulated flows from the Abatzoglou-forced model closely correspond with the Elsner-Littell  
527 optimal calibrated flows (red line). Using an analogous comparison, it appears that the Maurer  
528 and Wood-Lettenmaier datasets yield similar flows, as seen in the panel third from left, where  
529 the flows resulting from the Abatzoglou-forced model closely correspond with the Maurer  
530 optimal calibrated flows.

531 For the SACRB and SALTC watersheds, it appears that simulated flows using a model  
532 forced by the Elsner-Littell dataset differs noticeably from others. In the top left panel,  
533 simulated flows using the Elsner-Littell calibrated model and forced with alternate datasets all  
534 show significantly lower mean seasonal peaks. Similarly, results from each of the other  
535 calibrated models show the Elsner-Littell forced flows have significantly higher seasonal peaks.

536 For the SNAKE watershed, it appears that simulated flows using a model forced by the  
537 Maurer dataset differs noticeably from others, similarly to the comparison described above for  
538 SACRB and SALTC. Unique differences in mean monthly hydrographs for each basin suggest  
539 that there may be compounding effects of forcing dataset, model calibration, and physical  
540 representation of important watershed processes.

#### 541 *4.3 Sensitivity of the Portrayal of Climate Impacts to Calibrated Parameters*

542 In a final analysis, we evaluate the sensitivity of runoff change to observed historical changes in  
543 precipitation and temperature (combined) using calibrated models forced with the four  
544 meteorological datasets in attempt to differentiate changes in sensitivity due to changes in

545 climate and to choice of dataset. Figure 10 summarizes the results for each case study  
546 watershed, with panels ordered column wise by lowest mean elevation (SACRB) to highest mean  
547 elevation (ANIMS). Each panel shows change in mean annual water year precipitation (percent)  
548 versus change in mean annual runoff (percent) between the calibration period and select years in  
549 the validation period. The size of each plotted symbol represents the corresponding magnitude  
550 (absolute value) of change in annual temperature (degrees C). The diamonds in each figure  
551 panel correspond with cool-wet validation years, while circles correspond with warm-dry  
552 validation years. Individual points represent results for one calibrated model simulation  
553 corresponding with the forcing dataset used for calibration. For all basins but MISSO and  
554 ANIMS, the computed change in precipitation between calibration years and cool-wet validation  
555 years is generally positive, while the change between calibration and warm-wet validation years  
556 is generally negative.

557 Figure 10 illustrates that precipitation is the primary driver of runoff change, which is  
558 consistent with conclusions of Matera et al. (2009), Nasonova et al. (2011), and Xue et al.  
559 (1991). Generally, increases in precipitation correspond with greater increases in runoff, similar  
560 to findings by Elsner et al. (2010) and Vano et al. (2012) which indicate about a 12-20% increase  
561 and a 20-30% increase in runoff for a 10% increase in precipitation for watersheds in  
562 Washington and the Colorado River basin, respectively.

563 The figure also shows that precipitation change and corresponding changes in runoff can  
564 be substantially different between datasets, on the order of, or greater than, projected changes in  
565 precipitation by the 2050s. The expectation would be that changes in precipitation and runoff  
566 from different calibrated models (and correspondingly different meteorological forcings) would  
567 cluster in two distinct groups corresponding to warm-dry and cool-wet regimes. Such clustering

568 is evident for the SACRB, for example. However, some watersheds have substantial differences  
569 (SALTC, for example), indicating that the choice of meteorological dataset may be as important  
570 in characterizing changes in runoff as is climate change.

571 Anomalies to the above generalizations regarding changes between calibration years and  
572 select validation years exist for the MISSO and ANIMS watersheds. In the MISSO watershed,  
573 the computed change in precipitation is positive between calibration years and both sets of  
574 validation years. For this watershed, as noted previously in the comparison of forcing datasets,  
575 all validation years were wetter than the calibration years, hence showing positive change  
576 precipitation, even in so-called warm-dry years (see also Fig. 8). For the ANIMS watershed, no  
577 validation years were classified as cool-wet for the Abatzoglou or Maurer datasets, so changes  
578 could not be computed. Plotted changes in precipitation and temperature for cool-wet validation  
579 years for the Elsner-Littell and Wood-Lettenmaier datasets show slightly less precipitation (by  
580 approximately 3 percent), despite the cool-wet classification, along with negative and positive  
581 changes in runoff (respectively). We speculate that the increased runoff with reduced  
582 precipitation, computed for the simulations using the Wood-Lettenmaier dataset, is an anomalous  
583 result of averaging mean annual values across select validation years.

## 584 5. Discussion

585 By comparing four spatially distributed meteorological forcing datasets and conducting  
586 experiments based on combinations of forcings and calibrated VIC hydrologic models, we seek  
587 to determine whether there is an optimal forcing dataset to be used by hydrologic models to  
588 simulate streamflow, and whether the choice of dataset affects VIC model calibration and  
589 portrayal of climate sensitivity.

590           The meteorological datasets considered (Abatzoglou, Elsner-Littell, Maurer, Wood-  
591 Lettenmaier) have substantial differences, particularly in minimum and maximum temperatures  
592 in higher elevation regions, which are primarily attributed to the approach taken to adjust  
593 temperature by elevation when interpolating station data to a grid. Temperature influences  
594 derived forcings within the VIC hydrologic model, such as radiation, and, consequently, the  
595 accumulation and ablation of the mountain snowpack. Therefore differences in minimum and  
596 maximum temperature may significantly affect the simulated water balance.

597           The temperature differences among meteorological forcing datasets are generally larger  
598 than the differences between calibration and validation periods. For precipitation, the differences  
599 among datasets are comparable with differences between calibration and validation periods, with  
600 the exception of the MISSO basin where the calibration and validation periods differ by 18-20%.

601           Although there are substantial differences among these datasets, no single dataset is  
602 superior to the others with respect to VIC simulations of streamflow. Also, there is no apparent  
603 relationship between optimal calibration parameter values and meteorological dataset or  
604 watershed, suggesting that the quality of the datasets is comparable or there is enough flexibility  
605 in the model parameters to compensate for differences among forcing datasets and potential  
606 biases in process representation.

607           The model calibration analysis shows that choice of forcing dataset influences VIC model  
608 calibration with respect to calibration parameters and resulting streamflow, in particular seasonal  
609 streamflow peaks. For example, in the ANIMS watershed, the Abatzoglou dataset results in  
610 better model performance according to the chosen calibration metrics, even when the model was  
611 calibrated to another dataset. In the SACRB watershed, the Elsner-Littell dataset results in  
612 significantly different mean monthly hydrographs than models using other datasets.

613 Finally, regarding exploration of runoff sensitivity to portrayal of climate impacts, we  
614 find that precipitation change and corresponding changes in runoff can be substantially different  
615 between datasets, on the order of, or greater than, projected climate change by the 2050s. This  
616 indicates that the choice of meteorological dataset may be as important in characterizing changes  
617 in runoff as climate change. Further, choice of meteorological forcing dataset will influence  
618 statistical downscaling of projected climate scenarios from coarser scale (in space and time)  
619 GCMs, thereby influencing the uncertainty associated with downscaled climate projections.

620 This work supports previous findings, suggesting that there are significant differences in  
621 meteorological forcing datasets, downscaling of global climate projections, hydrologic model  
622 constructs, and model calibration schemes, all of which may impact the portrayal of climate  
623 change impacts in long term natural resources planning studies. This work, along with other  
624 mentioned studies, supports the argument that consideration of uncertainties in modeling  
625 frameworks is as important as consideration of an ensemble of future climate projections in long-  
626 term planning studies. Further studies exploring the sensitivity of other hydrologic variables  
627 beyond streamflow (i.e. snowpack, evapotranspiration, etc.) to choice of meteorological forcing  
628 dataset, changes in runoff sensitivity due to hydrologic model calibration, as well as studies  
629 using ensembles of approaches and techniques (including additional hydrologic models), will  
630 enhance understanding of uncertainties and are critical for identifying best practices for  
631 applications.

632

### 633 *Acknowledgments*

634 The authors would like to thank Dr. Alan Hamlet (Assistant Professor at University of Notre  
635 Dame) and Dr. Andrew Wood (Research Scientist, NCAR Research Applications Laboratory)

636 for their insights into the development of the meteorological forcing datasets, as well as  
637 collaborators at the National Center for Atmospheric Research (Ethan Gutmann and Pablo  
638 Mendoza) for their constructive comments in the later stages of this study. The authors would  
639 also like to thank two anonymous reviewers for their valuable comments. Finally, the authors  
640 would like to acknowledge the Bureau of Reclamation Research and Development Office for  
641 financially supporting this study.

642

## 643 **References**

- 644 Abatzoglou, J. T. 2011: Development of gridded surface meteorological data for ecological  
645 applications and modeling. *Int. J. Climatol.*, **33**, 121–131.
- 646 Barsugli, J.J., M.M. Elsner, and A.F. Hamlet, 2012. *Building a Stronger and More Extensive*  
647 *Hydrologic Foundation for Environmental Flow and Climate Change Research Across the*  
648 *Colorado River Basin*. Final project report, prepared for The Nature Conservancy.
- 649 Bennett, K.E., A.T. Werner, M. Schnorbus. 2012: Uncertainties in Hydrologic and Climate  
650 Change Impact Analyses in Headwater Basins of British Columbia. *J. Climate*, **25**, 5711–5730.
- 651 Bentz, B.J., J. Régnière, C.J. Fettig, E.M. Hansen, J.L. Hayes, J.A. Hicke, R.G. Kelsey, J.F.  
652 Negrón, and S.J. Seybold. 2010. Climate change and bark beetles of the western United States  
653 and Canada: direct and indirect effects. *BioScience*, 60 (8), 602-613..
- 654 Blandford, T. R., K. S. Humes, B. J. Harshburger, B. C. Moore, V. P. Walden, and H. Ye, 2008:  
655 Seasonal and Synoptic Variations in Near-Surface Air Temperature Lapse Rates in a  
656 Mountainous Basin, *Journal of Applied Meteorology and Climatology*, 47, 249-261.
- 657 Bohn, T. J., B. Livneh, J. W. Oyler, S. W. Running, B. Nijssen, and D. P. Lettenmaier, 2013:  
658 Global evaluation of MTCLIM and related algorithms for forcing of ecological and hydrological  
659 models, *Agric. For. Meteorol.*, **176**, 38-49.
- 660 Christensen N. and D.P. Lettenmaier, 2007: A multimodel ensemble approach to assessment of  
661 climate change impacts on the hydrology and water resources of the Colorado River basin.  
662 *Hydrol. Earth System Sci.*, **11**, 1417-1434
- 663 Clark, M. P., A. G. Slater, D. E. Rupp, R. A. Woods, J. A. Vrugt, H. V. Gupta, T. Wagener, and  
664 L. E. Hay, 2008: Framework for Understanding Structural Errors (FUSE): A modular framework  
665 to diagnose differences between hydrological models. *Water Resour. Res.*, **44**, W00B02.

666 Daly, C., M. Halbleib, J.I. Smith, W.P. Gibson, M.K. Doggett, G.H. Taylor, J. Curtis, and P.A.  
667 Pasteris, 2008: Physiographically-sensitive mapping of temperature and precipitation across the  
668 conterminous United States. *Int. J. Climatol.*, **28**, 2031-2064.

669 Elsner, M.M., L. Cuo, N. Voisin, J.S. Deems, A.F. Hamlet, J.A. Vano, K.E.B. Mickelson, S.Y.  
670 Lee, and D.P. Lettenmaier, 2010: Implications of 21st Century climate change for the hydrology  
671 of Washington State. *Climatic Change*, **102 (1-2)**, 225-260.

672 Gangopadhyay, S., M. Clark, K. Werner, D. Brandon, and B. Rajagopalan, 2004: Effects of  
673 Spatial and Temporal Aggregation on the Accuracy of Statistically Downscaled Precipitation  
674 Estimates in the Upper Colorado River Basin. *J. Hydrometeorol.*, **5**, 1192–1206.

675 Guo, Z., P. A. Dirmeyer, Z.-Z. Hu, X. Gao, and M. Zhao, 2006: Evaluation of the Second Global  
676 Soil Wetness Project soil moisture simulations: 2. Sensitivity to external meteorological forcing.  
677 *J. Geophys. Res.: Atmos.*, **111**, n/a-n/a.

678 Hamlet, A. F. and D. P. Lettenmaier, 2005: Production of temporally consistent gridded  
679 precipitation and temperature fields for the continental U.S. *J. Hydrometeorol.*, **6 (3)**, 330-336.

680 Hamlet, A. F., M.M. Elsner, G. Mauger, S. Y. Lee, and I. M. Tohver, 2013: An Overview of the  
681 Columbia Basin Climate Change Scenarios Project: Approach, Methods, and Summary of Key  
682 Results. *Atmos.-Ocean*, **51(4)**, 392-415.

683 Hay, L. E., R. L. Wilby, and G. H. Leavesley, 2000: A COMPARISON OF DELTA CHANGE  
684 AND DOWNSCALED GCM SCENARIOS FOR THREE MOUNTAINOUS BASINS IN THE  
685 UNITED STATES. *J. Amer. Water Resour. Assoc.*, **36**, 387–397.

686 Hay, L.E., G. H. Leavesley, M. P. Clark, S. L. Markstrom, R. J. Viger, and M. Umemoto, 2006:  
687 Step Wise, Multiple Objective Calibration of a Hydrologic Model for a Snowmelt Dominated  
688 Basin. *J. Amer. Water Res. Assoc.*, **42**, 877–890.

689 Hossain, F., and E.N. Anagnostou. (2005). Numerical investigation of the impact of uncertainties  
690 in satellite rainfall estimation and land surface model parameters on simulation of soil moisture.  
691 *Advances in Water Res.*, **28** (12), 1336-1350.

692 Kalanay, E., M. Kanamitsu, R. Kistler, W. Collins, D. Deaven, L. Gandin, M. Iredell, S. Saha, G.  
693 White, J. Woollen, Y. Zhu, A. Leetmaa, and R. Reynolds, M. Chelliah, W. Ebisuzaki, W.  
694 Higgins, J. Janowiak, K. C. Mo, C. Ropelewski, and J. Wang, R. Jenne, and D. Joseph, 1996:  
695 The NCEP/NCAR 40-year reanalysis project. *Bull. Amer. Meteor. Soc.* **77**, 437–471.

696 Kampf, S. K., and S. J. Burges 2007: A framework for classifying and comparing distributed  
697 hillslope and catchment hydrologic models. *Water Resour. Res.*, **43**, W05423.

698 Liang X, E. F. Wood, D. P. Lettenmaier, 1996: Surface soil moisture parameterization of the  
699 VIC-2L model: evaluation and modifications. *Glob. Planet Change*, **13**, 195–206.

700 Littell, J. S., M. M. Elsner, G. S. Mauger, E. R. Lutz, A. F. Hamlet, and E. P. Salathé. 2011:  
701 *Regional Climate and Hydrologic Change in the Northern U.S. Rockies and Pacific Northwest:*  
702 *Internally Consistent Projections of Future Climate for Resource Management*. Preliminary  
703 project report, USFS JVA 09-JV-11015600-039. Prepared by the Climate Impacts Group,  
704 University of Washington, Seattle.

705 Livneh B, E.A. Rosenberg, C. Lin, B. Nijssen, V. Mishra, K. Andreadis, E.P. Maurer, and D.P.  
706 Lettenmaier, 2013: A long-term hydrologically based data set of land surface fluxes and states  
707 for the conterminous United States: Updates and extensions. *J. Climate*, (in review).

708 Lohmann, D., E. Raschke, B. Nijssen, and D.P. Lettenmaier, 1998: Regional scale hydrology: I.  
709 Formulation of the VIC-2L model coupled to a routing model. *Hydrol. Sci. J.*, **43**, 131-141.

710 Maggioni, V., E. N. Anagnostou, and R. H. Reichle.(2012) The impact of model and rainfall  
711 forcing errors on characterizing soil moisture uncertainty in land surface modeling. *Hydrol.*  
712 *Earth Sys. Sci.* **16 (10)**, 3499-3515.

713 Materia, S., P. A. Dirmeyer, Z. Guo, A. Alessandri, A. Navarra, 2010: The Sensitivity of  
714 Simulated River Discharge to Land Surface Representation and Meteorological Forcings. *J.*  
715 *Hydrometeor.*, **11**, 334–351.

716 Maurer, E.P., A. W. Wood, J. C. Adam, D. P. Lettenmaier, and B. Nijssen, 2002: A long-term  
717 hydrologically-based data set of land surface fluxes and states for the conterminous United  
718 States. *J. Climate*, **15**, 3237-3251.

719 Maurer, E. P., L. Brekke, T. Pruitt, and P. B. Duffy, 2007: Fine-resolution climate projections  
720 enhance regional climate change impact studies. *Eos Trans. AGU*, **88(47)**, 504-504.

721 McKelvey, K.S., J.P. Copeland, M.K. Schwartz, J.S. Littell, K.B. Aubry, J.R. Squires, S.A.  
722 Parks, M.M. Elsner, and G.S. Mauger, 2011: Climate change predicted to shift wolverine  
723 distributions, connectivity, and dispersal corridors. *Ecol. Appl.*, **21(8)**, 2882-2897.

724 Meehl, G. A., C. Covey, T. Delworth, M. Latif, B. McAvaney, J. F. B. Mitchell, R. J. Stouffer,  
725 and K. E. Taylor, 2007: The WCRP CMIP3 multi-model dataset: A new era in climate change  
726 research. *Bull. Amer. Meteor. Soc.*, **88**, 1383-1394.

727 Merz, R., J. Parajka, and G. Blöschl, 2011: Time stability of catchment model parameters:  
728 Implications for climate impact analyses. *Water Resour. Res.*, **47**, W02531.

729 Mesinger, F, G. DiMego, E. Kalnay, K. Mitchell, P. C. Shafran, W. Ebisuzaki, D. Jović, J.  
730 Woollen, E. Rogers, E. H. Berbery, M. B. Ek, Y. Fan, R. Grumbine, W. Higgins, H. Li, Y. Lin,  
731 G. Manikin, D. Parrish, and W. Shi, 2006: North American Regional Reanalysis. *Bull. Amer.*  
732 *Meteor. Soc.*, **87**, 343–360.

733 Mitchell, K.E., D. Lohmann, P.R. Houser, E.F. Wood, J.C. Schaake, A. Robock, B.A. Cosgrove,  
734 J. Sheffield, Q. Duan, L. Luo, R.W. Higgins, R.T. Pinker, J.D. Tarpley, D.P. Lettenmaier, C.H.  
735 Marshall, J.K. Entin, M. Pan, W. Shi, V. Koren, J. Meng, B. H. Ramsay, and A.A. Bailey, 2004:  
736 The multi-institution North American Land Data Assimilation System (NLDAS): Utilizing  
737 multiple GCIP products and partners in a continental distributed hydrological modeling system.  
738 *J. Geophys. Res.*, **109**, D07S90.

739 Mizukami, N., M. P., Clark, A. Slater, L. Brekke, M. M. Elsner, J. Arnold, S. Gangopadhyay,  
740 2013: Evaluation of different methods to construct large-scale hydrologic model forcing data in  
741 mountainous regions. *J. Hydrometeorol.*, **15**, 474–488.

742 Mo, K. C., L.-C. Chen, S. Shukla, T. J. Bohn, and D. P. Lettenmaier, 2012: Uncertainties in  
743 North American Land Data Assimilation Systems over the Contiguous United States. *J.*  
744 *Hydrometeorol.*, **13**, 996-1009.

745 Nasonova, O. N., Y. M. Gusev, and Y. E. Kovalev, 2011: Impact of uncertainties in  
746 meteorological forcing data and land surface parameters on global estimates of terrestrial water  
747 balance components. *Hydrol. Proc.*, **25**, 1074-1090.

748 Reclamation, 2011: *West-Wide Climate Risk Assessments: Bias-Corrected and Spatially*  
749 *Downscaled Surface Water Projections, Technical Memorandum No. 86-68210-2011-01*,  
750 prepared by the U.S. Department of the Interior, Bureau of Reclamation, Technical Services  
751 Center, Denver, Colorado. 138pp.

752 Salathé, E.P., P.W. Mote, and M.W. Wiley, 2007: Review of scenario selection and downscaling  
753 methods for the assessment of climate change impacts on hydrology in the United States Pacific  
754 Northwest. *Int. J. of Climatol.*, **27(12)**, 1611-1621.

755 Shepard, D.S.,1984: Computer mapping: the SYMAP interpolation algorithm. In: Willmott GL,

756 Reidel CJ (eds) *Spatial statistics and Models* Gaille, pp 133–145.

757 Thornton, P. E., and S. W. Running, 1999: An improved algorithm for estimating incident daily  
758 solar radiation from measurements of temperature, humidity, and precipitation, *Agric. For.*  
759 *Meteorol.*, **93**, 211 –228.

760 Vano, J. A., T. Das, and D. P. Lettenmaier, 2012: Hydrologic sensitivities of Colorado River  
761 runoff to changes in precipitation and temperature, *J. Hydrometeorol.*, **13(3)**, 932-949.

762 Vaze, J., D. A. Post, F. H. S. Chiew, J.-M. Perraud, N. R. Viney, and J. Teng, 2010: Climate  
763 non-stationarity – Validity of calibrated rainfall–runoff models for use in climate change studies,  
764 *J. Hydrol.*, **394(3–4)**, 447-457.

765 Wenger, S. J., D. J. Isaak, C. H. Luce, H. M. Neville, K. D. Fausch, J. B. Dunham, D.C.

766 Dauwalter, M. K. Young, M. M. Elsner, B. E. Rieman, A. F. Hamlet, and J. E. Williams, 2011:  
767 Flow regime, temperature and biotic interactions drive differential declines of trout species under  
768 climate change. *Proc. Natl. Acad. Sci. U. S. A.*, **108(34)**, 14175-14180.

769 Wilby, R. L. 2005: Uncertainty in water resource model parameters used for climate change  
770 impact assessment. *Hydrol. Process.*, **19**, 3201–3219.

771 Wood, A.W., L. R. Leung, V. Sridhar and D. P. Lettenmaier, 2004: Hydrologic implications of  
772 dynamical and statistical approaches to downscaling climate model outputs, *Climatic Change*,  
773 **62(1-3)**, 189-216.

774 Wood, A. W. and D.P. Lettenmaier, 2006: A testbed for new seasonal hydrologic forecasting  
775 approaches in the western U.S. *Bull. Amer. Meteor. Soc.*, **87(12)**, 1699-1712.

776 Wood, A. W. 2008: The University of Washington Surface Water Monitor: An experimental  
777 platform for national hydrologic prediction, *Proc. Amer. Meteor. Soc. Annual Meeting, New*  
778 *Orleans*, 13 p.

779 Xia, Y., K. Mitchell, M. Ek, J. Sheffield, B. Cosgrove, E. Wood, L. Luo, C. Alonge, H. Wei, J.  
780 Meng, B. Livneh, D. Lettenmaier, V. Koren, Q. Duan, K. Mo, Y. Fan, D. Mocko, 2012:  
781 Continental-scale water and energy flux analysis and validation for North American Land Data  
782 Assimilation System project phase 2 (NLDAS-2): 2. Validation of model-simulated streamflow.  
783 *J. Geophys. Res.*, **117**, D03110.

784 Xue, Y., P. J. Sellers, J. L. Kinter, and J. Shukla, 1991: A simplified biospheremodel for global  
785 climate studies. *J. Climate*, **4**, 345–364.

786 Yapo, P.O., Hoshin Vijai Gupta, Soroosh Sorooshian (1998). Multi-objective global optimization  
787 for hydrologic models. *J. Hydrol.*, **204(1–4)**, 83–97.

788

789 **Tables**

790 TABLE 1. Summary of differences in development of spatially distributed meteorological  
 791 datasets. Notes: HCN is Historical Climatology Network; AHCCD is Adjusted Historical  
 792 Canadian Climate Database; Prcp is precipitation; Tmax is maximum temperature; Tmin is  
 793 minimum temperature; CONUS is continental United States; PRISM is Parameter-elevation  
 794 Regressions on Independent Slopes Model.

<b>Name</b>	<b>References</b>	<b>Spatial Extent</b>	<b>Native Spatial Resolution</b>	<b>Temporal Coverage</b>	<b>Distinguishing Characteristics</b>
<b>Maurer (M)</b>	Maurer et al. 2002	CONUS plus Canadian portions of Columbia and Missouri basins	1/8 degree	1949-2000	Gridded Co-op station data (w/ more than 20 years data); Prcp scaled to PRISM climatology (1961-1990); Temp lapsed to grid cell elevation (-6.5degrees C per km);
<b>Wood-Lettenmaier (WL)</b>	Wood and Lettenmaier 2006; Wood (2008)	Major Western US watersheds, including Canadian portions	1/8 degree	1915-2005	Gridded Co-op station data (w/ more than 45 years data and 80% coverage); Index Station Method applied to data post 2004; Prcp scaled to PRISM climatology (1961-1990); Temp lapsed to grid cell elevation (-6.5degrees C per km);
<b>Abatzolou (A)</b>	Abatzoglou 2011	CONUS	4-km	1979-2010	NLDAS Phase 2 – Prcp, Tmin, Tmax interpolated & scaled to PRISM monthly timeseries
<b>Elsner-Littell (EL)</b>	Elsner et al. 2010; Littell et al. 2011	Major Western US watersheds, including Canadian portions	1/16 degree	1915-2006	Gridded Co-op station data (w/ more than 5 years data); HCN and AHCCD station data used to correct temporal inhomogeneities; Temp lapsed to grid cell elevation (-6.5degrees C per km); Prcp & Tavg scaled to PRISM climatology (1971-2000).

795 TABLE 2. Summary of VIC model parameters considered for calibration. Parameters were  
 796 evaluated using perturbation experiments and those chosen for calibration are noted by “X”.

<b>Considered Model Calibration Parameters</b>	<b>Parameter Units</b>	<b>Description</b>	<b>Parameter Range</b>	<b>Sensitive</b>
bi	NA	Variable infiltration curve parameter	0 - 0.4	
Ds	fraction	Fraction of Dsmax where nonlinear baseflow occurs	0.00001 - 1	X
Dsmax	mm/day	Maximum velocity of baseflow	0.1 - 30	X
Ws	fraction	Fraction of max. soil moisture where nonlinear baseflow occurs	0.05 - 1	X
D2	mm	Middle soil depth	0.1 - 1.0	X
D3	mm	Lowest soil depth	0.5 - 2.5	X
wind_atten	fraction	Defines windspeed profile through canopy	0 - 1	
snow_rough	m	Surface roughness of snowpack	0 - 1	
rad_atten	fraction	Defines shortwave radiation through canopy	0.1 - 0.6	
Velocity	m/s	streamflow routing velocity	0.5 - 2.5	

797

798 TABLE 3. Summary of case study watersheds.

Name (ID)	Description	Size, sqkm (No. VIC cells)	Calibration Period (water years)	Validation Period (water years)	Mean Annual P (mm)	Mean Annual T (deg C)	Mean Annual Flow (cms)
ANIMS (1)	Animas River at Durango, CO (USGS ID 09361500)	1792 (21)	1993-1999	1986-1992	900 - 978	0.7 - 2.3	24
DOLOR (2)	Dolores River near Cisco, UT (USGS ID 09180000)	11,862 (103)	1990-1999	1980-1989	552 - 591	6.0 - 6.9	38
GREEN (3)	Green River at Green River, UT (USGS ID 09315000)	116,162 (816)	1990-1999	1980-1989	423 - 450	4.0 - 5.1	226
MISSO (4)	Missouri River at Toston, MT (USGS ID 06054500)	39,993 (346)	1985-1989	1980-1984	589 - 644	2.5 - 3.4	189
SACRB (5)	Sacramento River at Bend Bridge near Red Bluff, CA (USGS ID 11377200)	23,051 (230)	1990-1999	1980-1989	888 - 958	8.6 - 9.8	351
SALTC (6)	Salt River near Chrysotile, AZ (USGS ID 09497500)	7,379 (72)	1990-1999	1980-1989	603 - 643	9.7 - 9.8	23
SNAKE (7)	Snake River near Heise, ID (USGS ID 13037500)	14,898 (144)	1990-1999	1980-1989	825 - 897	0.4 - 2.1	208

799

800 TABLE 4. Summary of optimal VIC model calibration parameters according to meteorological  
801 dataset.

	<b>Name</b>	<b>Abatzoglou</b>	<b>Elsner-Littell</b>	<b>Maurer</b>	<b>Wood-Lettenmaier</b>
<b>Ds (fraction)</b>	ANIMS	0.00378	0.08373	0.99968	0.04988
	DOLOR	0.00283	0.01581	0.15324	0.00072
	GREEN	0.00961	0.01700	0.04588	0.02679
	MISSE	0.00922	0.01157	0.04193	0.02575
	SACRB	0.36768	0.32754	0.35505	0.39765
	SALTC	0.00295	0.00010	0.05496	0.07888
	SNAKE	0.02216	0.04806	0.50982	0.05335
	<b>Name</b>	<b>Abatzoglou</b>	<b>Elsner-Littell</b>	<b>Maurer</b>	<b>Wood-Lettenmaier</b>
<b>Ws (fraction)</b>	ANIMS	0.16129	0.36299	0.71606	0.12935
	DOLOR	0.53094	0.43526	0.51216	0.41465
	GREEN	0.51271	0.63571	0.78918	0.64319
	MISSE	0.15003	0.21649	0.38934	0.36493
	SACRB	0.93204	0.99933	0.99326	0.14904
	SALTC	0.60128	0.44716	0.50946	0.71447
	SNAKE	0.14693	0.25227	0.79960	0.48482
	<b>Name</b>	<b>Abatzoglou</b>	<b>Elsner-Littell</b>	<b>Maurer</b>	<b>Wood-Lettenmaier</b>
<b>Dsmax (mm/d)</b>	ANIMS	4.896	7.014	6.061	29.738
	DOLOR	14.710	5.539	3.511	27.741
	GREEN	4.367	4.624	1.658	2.264
	MISSE	25.537	24.344	6.713	7.378
	SACRB	3.073	3.244	2.630	0.603
	SALTC	17.930	0.878	29.179	1.240
	SNAKE	29.982	29.831	2.940	29.546
	<b>Name</b>	<b>Abatzoglou</b>	<b>Elsner-Littell</b>	<b>Maurer</b>	<b>Wood-Lettenmaier</b>
<b>D2 (mm)</b>	ANIMS	0.9955	0.9944	0.8166	0.9727
	DOLOR	0.9899	0.9998	0.9165	0.4979
	GREEN	0.9744	0.7994	0.8084	0.9682
	MISSE	0.9835	0.9988	0.9965	0.9963
	SACRB	0.3642	0.9633	0.2295	0.6505
	SALTC	0.5753	0.1748	0.9997	0.2929
	SNAKE	0.3403	0.4892	0.1002	0.2622
	<b>Name</b>	<b>Abatzoglou</b>	<b>Elsner-Littell</b>	<b>Maurer</b>	<b>Wood-Lettenmaier</b>
<b>D3 (mm)</b>	ANIMS	0.7107	1.1179	0.6296	1.4930
	DOLOR	1.3021	0.9797	0.5711	2.4071
	GREEN	1.1892	1.7170	2.1575	1.1475
	MISSE	2.4738	2.4913	1.7045	2.0047
	SACRB	1.5519	2.0709	1.7005	0.9533
	SALTC	0.7808	0.9315	0.5011	0.6348
	SNAKE	1.5616	1.2289	1.3075	1.1267

802

803 TABLE 5. Summary of VIC model calibration (validation) statistics according to calibration  
 804 parameter, watershed, and meteorological dataset.

	<b>Name</b>	<b>Abatzoglou</b>	<b>Elsner-Littell</b>	<b>Maurer</b>	<b>Wood-Lettenmaier</b>
<b>NSE<sub>mon</sub></b>	ANIMS	0.87 (0.78)	0.70 (0.75)	0.82 (0.73)	0.87 (0.80)
	DOLOR	0.78 (0.74)	0.76 (0.70)	0.76 (0.75)	0.78 (0.79)
	GREEN	0.95 (0.93)	0.89 (0.88)	0.94 (0.92)	0.93 (0.91)
	MISSE	0.74 (0.87)	0.69 (0.84)	0.80 (0.91)	0.80 (0.91)
	SACRB	0.95 (0.94)	0.92 (0.86)	0.92 (0.91)	0.94 (0.93)
	SALTC	0.85 (0.56)	0.84 (0.71)	0.77 (0.65)	0.83 (0.65)
	SNAKE	0.98 (0.91)	0.93 (0.86)	0.93 (0.87)	0.96 (0.95)
	<b>Name</b>	<b>Abatzoglou</b>	<b>Elsner-Littell</b>	<b>Maurer</b>	<b>Wood-Lettenmaier</b>
<b>RMSE<sub>mon</sub></b>	ANIMS	0.41 (0.48)	0.61 (0.51)	0.47 (0.56)	0.40 (0.46)
	DOLOR	0.62 (0.68)	0.65 (0.72)	0.65 (0.66)	0.63 (0.60)
	GREEN	0.25 (0.29)	0.35 (0.37)	0.27 (0.30)	0.28 (0.31)
	MISSE	0.33 (0.27)	0.36 (0.30)	0.29 (0.23)	0.29 (0.22)
	SACRB	0.24 (0.24)	0.29 (0.37)	0.29 (0.29)	0.25 (0.26)
	SALTC	0.58 (0.77)	0.60 (0.63)	0.72 (0.69)	0.62 (0.69)
	SNAKE	0.16 (0.28)	0.27 (0.34)	0.28 (0.33)	0.20 (0.20)
	<b>Name</b>	<b>Abatzoglou</b>	<b>Elsner-Littell</b>	<b>Maurer</b>	<b>Wood-Lettenmaier</b>
<b>VolErr<sub>mon</sub></b>	ANIMS	0.00 (0.01)	0.00 (0.02)	0.00 (0.26)	0.00 (0.01)
	DOLOR	0.21 (0.22)	0.00 (0.11)	0.21 (0.35)	0.03 (0.18)
	GREEN	0.00 (0.01)	0.01 (0.07)	0.00 (0.00)	0.00 (0.09)
	MISSE	0.00 (0.05)	0.00 (0.12)	0.00 (0.05)	0.00 (0.00)
	SACRB	0.00 (0.00)	0.00 (0.10)	0.00 (0.10)	0.05 (0.07)
	SALTC	0.01 (0.06)	0.00 (0.20)	0.00 (0.17)	0.01 (0.12)
	SNAKE	0.00 (0.02)	0.00 (0.03)	0.00 (0.13)	0.01 (0.04)

805

806

## 807 **List of Figures**

808 FIG 1. Overview map of study domain (2-digit HUC scale) and case study watersheds. Case  
809 study watersheds include: 1) Animas River at Durango, CO (USGS ID 09361500); 2) Dolores  
810 River near Cisco, UT (USGS ID 09180000); 3) Green River at Green River, UT (USGS ID  
811 09315000); 4) Missouri River at Toston, MT (USGS ID 06054500); 5) Sacramento River at  
812 Bend Bridge near Red Bluff, CA (USGS ID 11377200); 6) Salt River near Chrysotile, AZ  
813 (USGS ID 09497500); and, 7) Snake River near Heise, ID (USGS ID 13037500). The purple  
814 dashed line indicates the common domain used for meteorological dataset comparison.

815  
816 FIG 2. Percent differences of (A) annual means, (B) standard deviations, and (C) correlation  
817 coefficients between each of the three precipitation (Prcp) datasets (A = Abatzoglou;  
818 EL=Elsner-Littell; WL=Wood-Lettenmaier) and the reference dataset, i.e., Maurer et al.  
819 (2002). The boxes represent the 25th, 50th, 75th percentiles, while the whiskers represent the 5th  
820 and 95th percentiles. Light dashed lines represent change of +/-10 percent.

821  
822 FIG 3a-b. Spatial comparison of percent difference in monthly mean precipitation (Prcp) -  
823 January, top [A]; July, bottom [B]- comparing Wood-Lettenmaier, Elsner-Littell, and  
824 Abatzoglou datasets with respect to the Maurer dataset. Positive difference indicates higher  
825 monthly precipitation, while negative median difference indicates lower monthly precipitation.

826  
827 FIG 4. Percent differences of (A) annual means, (B) standard deviations, and (C) correlation  
828 coefficients between each of the three maximum temperature (Tmax) datasets (A = Abatzoglou;  
829 EL=Elsner-Littell; WL=Wood-Lettenmaier) and the reference dataset, i.e., Maurer et al.

830 (2002). The boxes represent the 25th, 50th, 75th percentiles, while the whiskers represent the 5th  
831 and 95th percentiles.

832

833 FIG 5. Percent differences of (A) annual means, (B) standard deviations, and (C) correlation  
834 coefficients between each of the three minimum temperature (Tmin) datasets (A = Abatzoglou;  
835 EL=Elsner-Littell; WL=Wood-Lettenmaier) and the reference dataset, i.e., Maurer et al.  
836 (2002). The boxes represent the 25th, 50th, 75th percentiles, while the whiskers represent the 5th  
837 and 95th percentiles.

838

839 FIG 6. Percent differences of (A) annual means, (B) standard deviations, and (C) correlation  
840 coefficients between each of the three diurnal temperature range (Tran) datasets (A =  
841 Abatzoglou; EL=Elsner-Littell; WL=Wood-Lettenmaier) and the reference dataset, i.e.,  
842 Maurer et al. (2002). The boxes represent the 25th, 50th, 75th percentiles, while the whiskers  
843 represent the 5th and 95th percentiles.

844

845 FIG 7a-b. Spatial comparison of difference (in degrees C) in monthly mean temperature  
846 (maximum [Tmax], minimum [Tmin], and diurnal range [Tran]) – January, top [A]; July, bottom  
847 [B] – comparing Wood-Lettenmaier, Elsner-Littell, and Abatzoglou datasets with respect to the  
848 Maurer dataset. Positive difference indicates high monthly temperature, while negative  
849 difference indicates lower monthly temperature.

850

851 FIG 8. Summary of differences in mean annual precipitation and temperature (Tavg, Tmax, and  
852 Tmin) between Abatzoglou, Elsner-Littell, Wood-Lettenmaier and the reference Maurer dataset.

853 Differences are shown over the seven case study watersheds and over 3 simulation periods: full  
854 simulation – 1980-1999 water years, calibration period, and validation period.

855

856 FIG 9. Summary of simulated flows based on calibrated models for seven case study watersheds  
857 (to each of the four meteorological forcing datasets) forced with alternate forcing datasets. In  
858 each figure panel, EL, A, M, and WL in the legend title (i.e. top row of legend above the line)  
859 indicate the base meteorological dataset used for model calibration. The black line represents  
860 mean monthly reconstructed natural streamflow at the watershed outlet. The red line represents  
861 resulting mean monthly streamflow from “base” calibrated simulations, having corresponding  
862 dataset and calibration parameters. The colored dashed lines represent mean monthly  
863 streamflow from simulations using calibrated parameters from the base simulation along with  
864 alternate meteorological datasets.

865

866 FIG 10. Change in mean annual precipitation (Prcp) vs. change in mean annual runoff (RO),  
867 computed between the calibration period and selected warm-dry years (circles) and cool-wet  
868 years (diamonds) in the validation period. Size of shapes represents the relative magnitude  
869 (absolute value) of corresponding change in mean annual temperature.

870

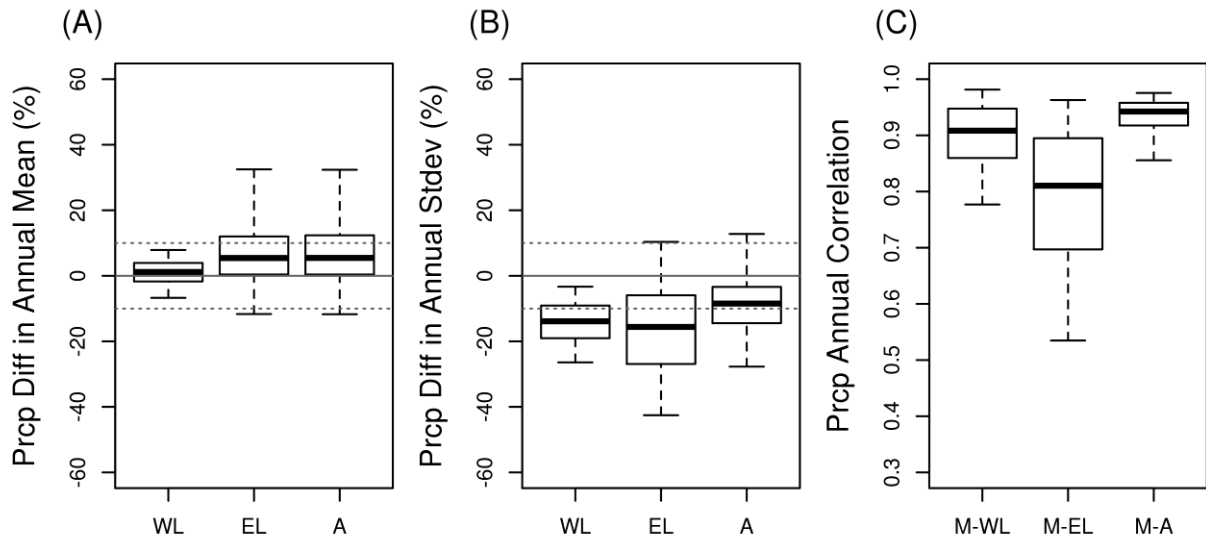
871 **Figures**

872 FIG 1. Overview map of study domain (2-digit HUC scale) and case study watersheds. Case  
873 study watersheds include: 1) Animas River at Durango, CO (USGS ID 09361500); 2) Dolores  
874 River near Cisco, UT (USGS ID 09180000); 3) Green River at Green River, UT (USGS ID  
875 09315000); 4) Missouri River at Toston, MT (USGS ID 06054500); 5) Sacramento River at  
876 Bend Bridge near Red Bluff, CA (USGS ID 11377200); 6) Salt River near Chrysotile, AZ  
877 (USGS ID 09497500); and, 7) Snake River near Heise, ID (USGS ID 13037500). The purple  
878 dashed line indicates the common domain used for meteorological dataset comparison.



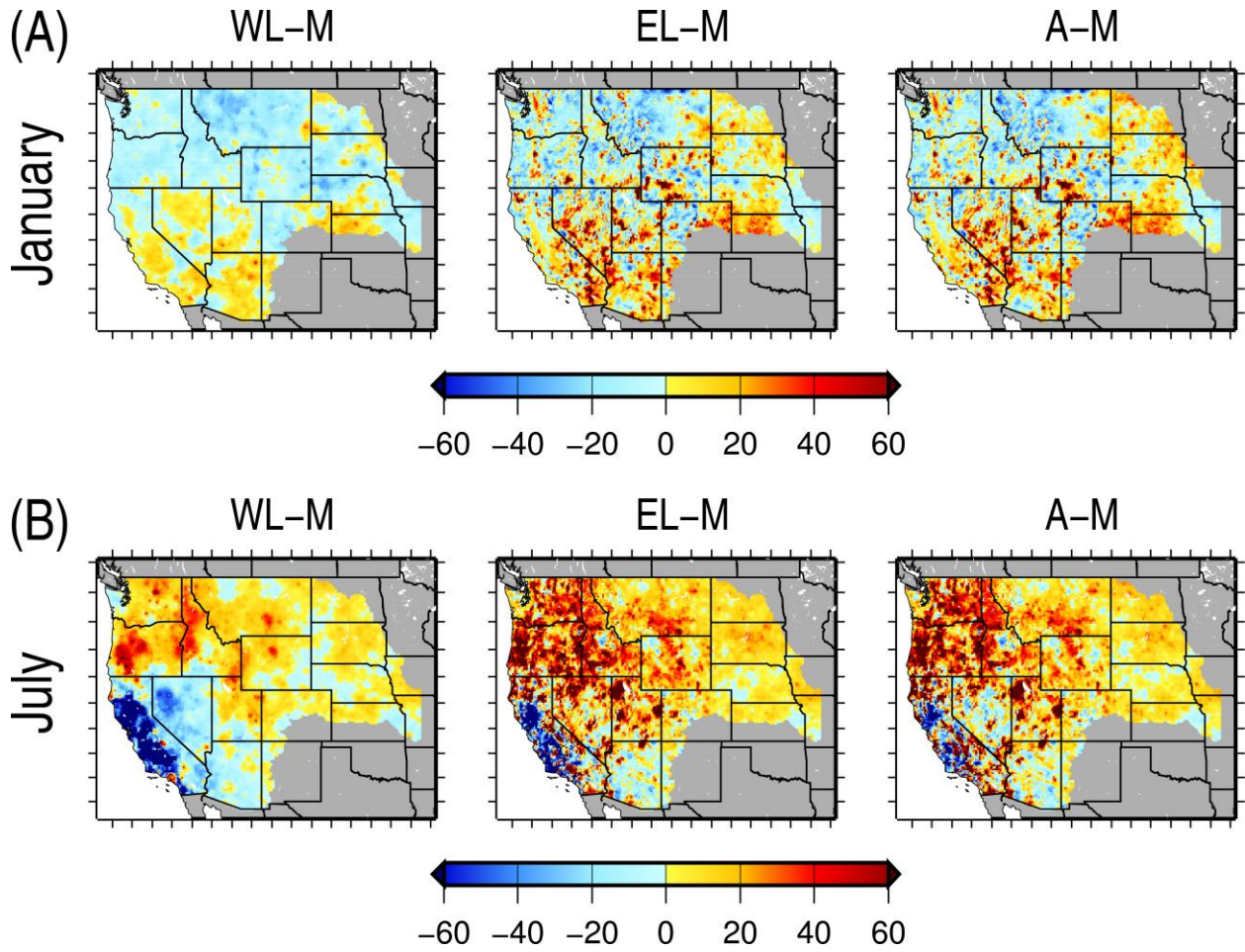
879

880  
881 FIG 2. Percent differences of (A) annual means, (B) standard deviations, and (C) correlation  
882 coefficients between each of the three precipitation (Prcp) datasets (A = Abatzoglou;  
883 EL=Elsner-Littell; WL=Wood-Lettenmaier) and the reference dataset, i.e., Maurer et al.  
884 (2002). The boxes represent the 25th, 50th, 75th percentiles, while the whiskers represent the 5th  
885 and 95th percentiles. Light dashed lines represent change of +/-10 percent.



886

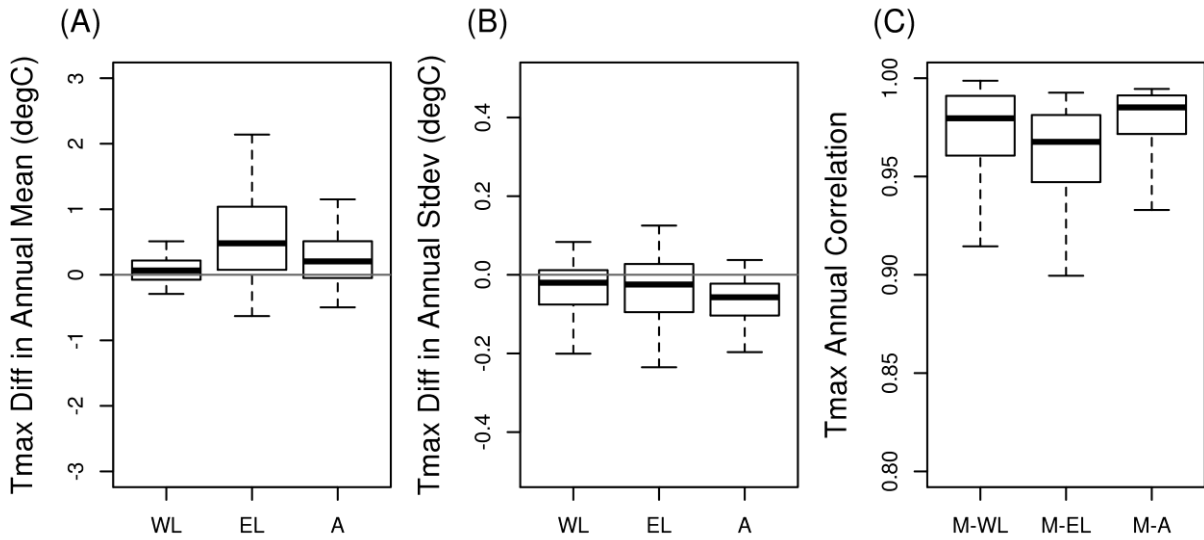
887 FIG 3a-b. Spatial comparison of percent difference in monthly mean precipitation (Prcp) -  
888 January, top [A]; July, bottom [B]- comparing Wood-Lettenmaier, Elsner-Littell, and  
889 Abatzoglou datasets with respect to the Maurer dataset. Positive difference indicates higher  
890 monthly precipitation, while negative median difference indicates lower monthly precipitation.



891

892

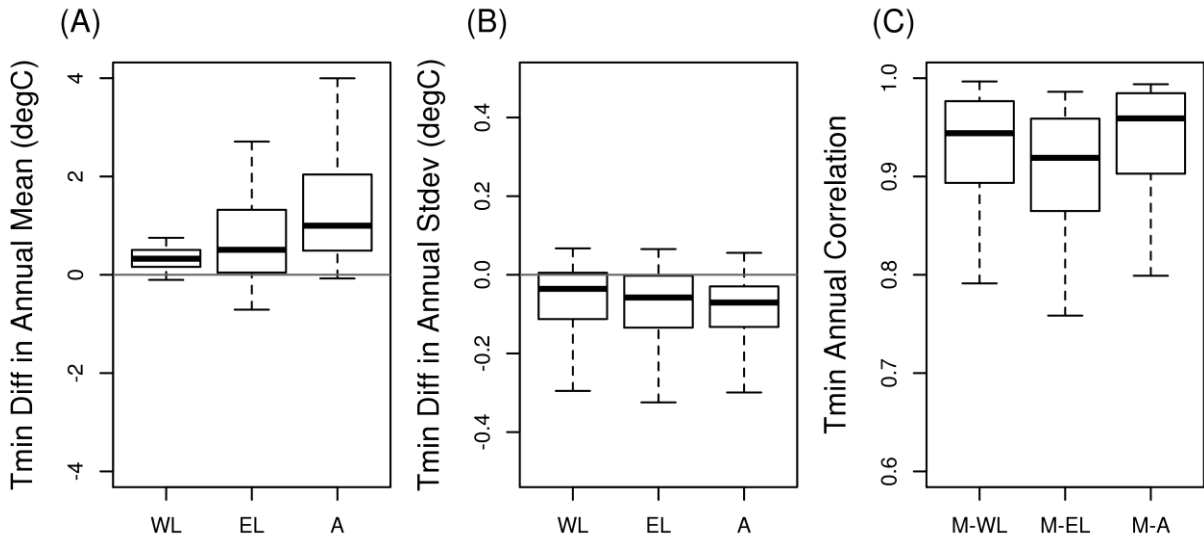
893 FIG 4. Percent differences of (A) annual means, (B) standard deviations, and (C) correlation  
 894 coefficients between each of the three maximum temperature (Tmax) datasets (A = Abatzoglou;  
 895 EL=Elsner-Littell; WL=Wood-Lettenmaier) and the reference dataset, i.e., Maurer et al.  
 896 (2002). The boxes represent the 25th, 50th, 75th percentiles, while the whiskers represent the 5th  
 897 and 95th percentiles.



898

899

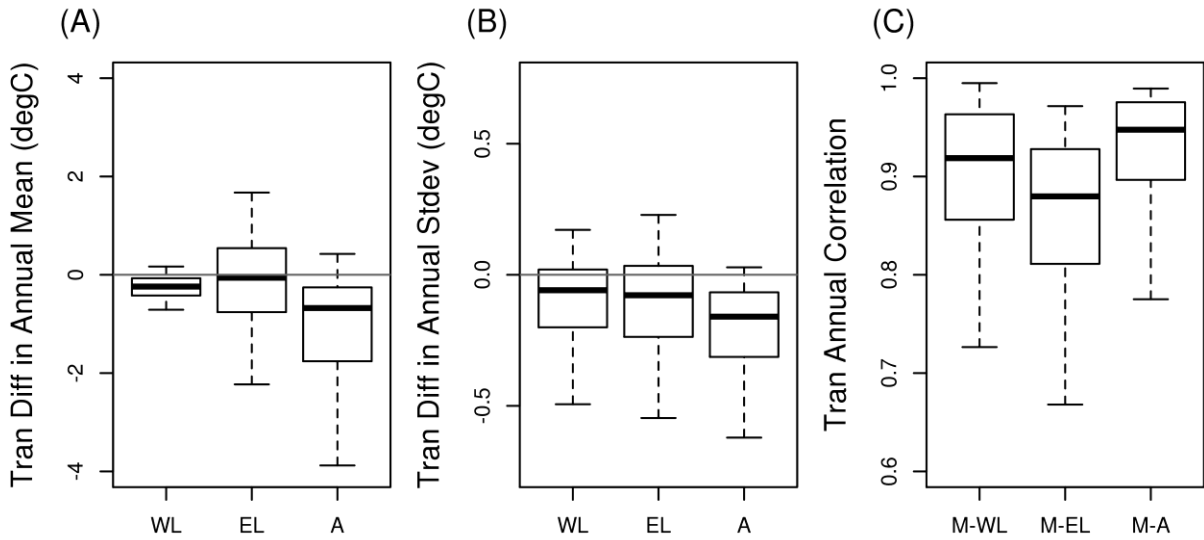
900 FIG 5. Percent differences of (A) annual means, (B) standard deviations, and (C) correlation  
901 coefficients between each of the three minimum temperature (Tmin) datasets (A = Abatzoglou;  
902 EL=Elsner-Littell; WL=Wood-Lettenmaier) and the reference dataset, i.e., Maurer et al.  
903 (2002). The boxes represent the 25th, 50th, 75th percentiles, while the whiskers represent the 5th  
904 and 95th percentiles.



905

906

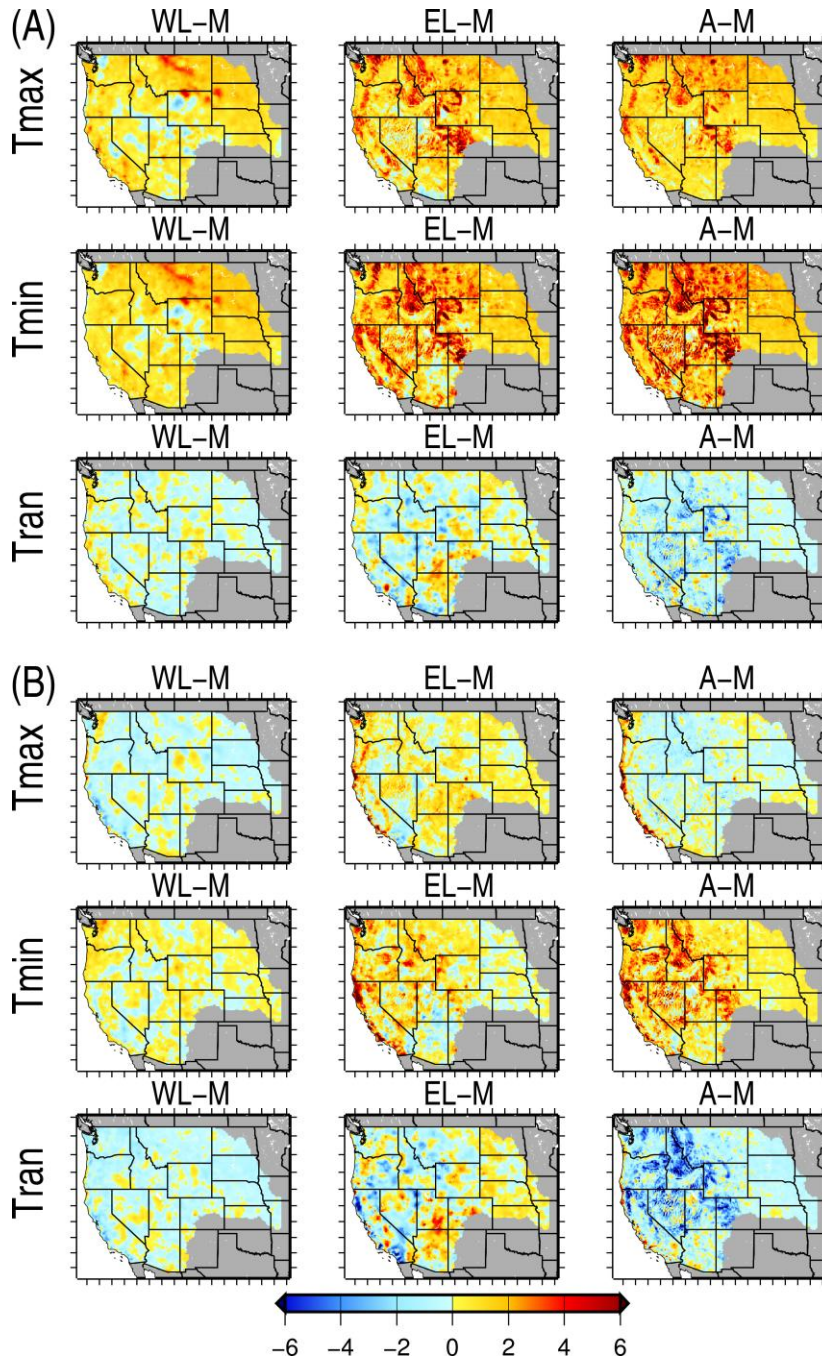
907 FIG 6. Percent differences of (A) annual means, (B) standard deviations, and (C) correlation  
 908 coefficients between each of the three diurnal temperature range (Tran) datasets (A =  
 909 Abatzoglou; EL=Elsner-Littell; WL=Wood-Lettenmaier) and the reference dataset, i.e.,  
 910 Maurer et al. (2002). The boxes represent the 25th, 50th, 75th percentiles, while the whiskers  
 911 represent the 5th and 95th percentiles.



912

913

914 FIG 7a-b. Spatial comparison of difference (in degrees C) in monthly mean temperature  
 915 (maximum [Tmax], minimum [Tmin], and diurnal range [Tran]) – January, top [A]; July, bottom  
 916 [B] – comparing Wood-Lettenmaier, Elsner-Littell, and Abatzoglou datasets with respect to the  
 917 Maurer dataset. Positive difference indicates high monthly temperature, while negative  
 918 difference indicates lower monthly temperature.



919

FIG 8. Summary of differences in mean annual precipitation and temperature (Tavg, Tmax, and Tmin) between Abatzoglou, Elsner-Littell, Wood-Lettenmaier and the reference Maurer dataset. Differences are shown over the seven case study watersheds and over 3 simulation periods: full simulation – 1980-1999 water years, calibration period, and validation period.

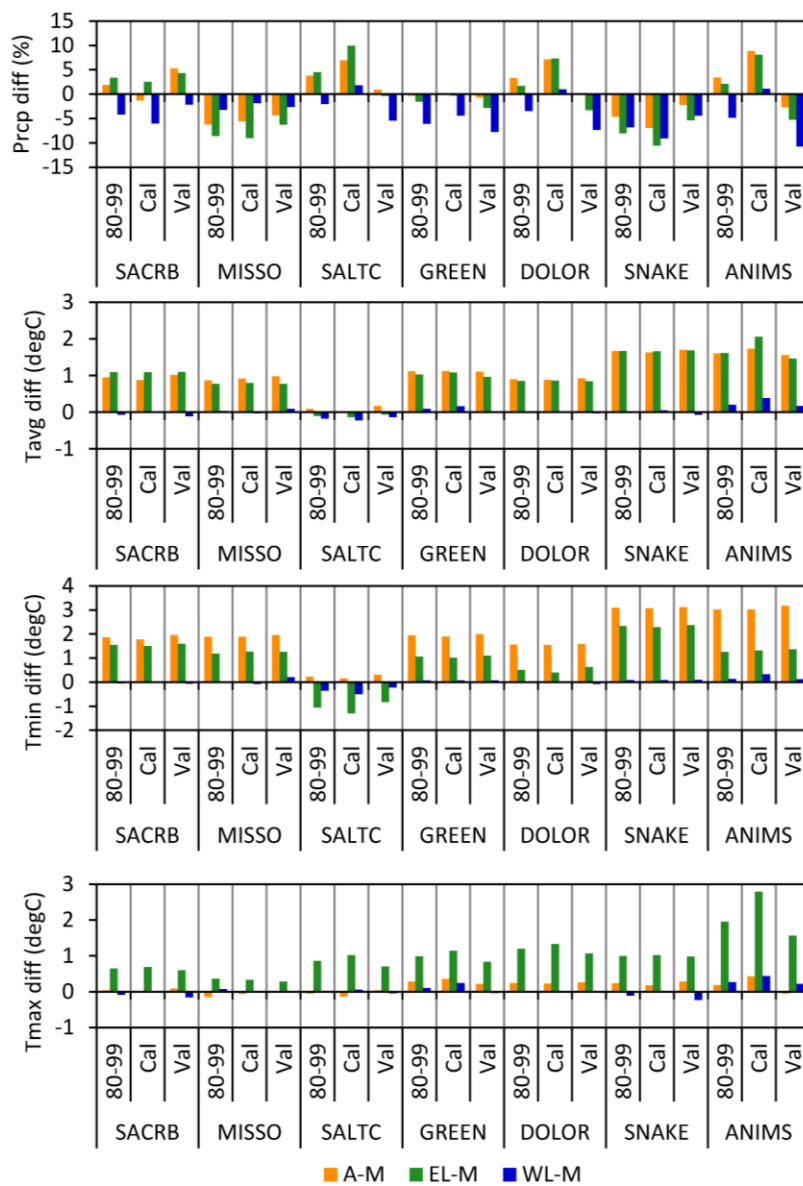


FIG 9. Summary of simulated flows based on calibrated models for seven case study watersheds (to each of the four meteorological forcing datasets) forced with alternate forcing datasets. In each figure panel, EL, A, M, and WL in the legend title (i.e. top row of legend above the line) indicate the base meteorological dataset used for model calibration. The black line represents mean monthly reconstructed natural streamflow at the watershed outlet. The red line represents resulting mean monthly streamflow from “base” calibrated simulations, having corresponding dataset and calibration parameters. The colored dashed lines represent mean monthly streamflow from simulations using calibrated parameters from the base simulation along with alternate meteorological datasets.

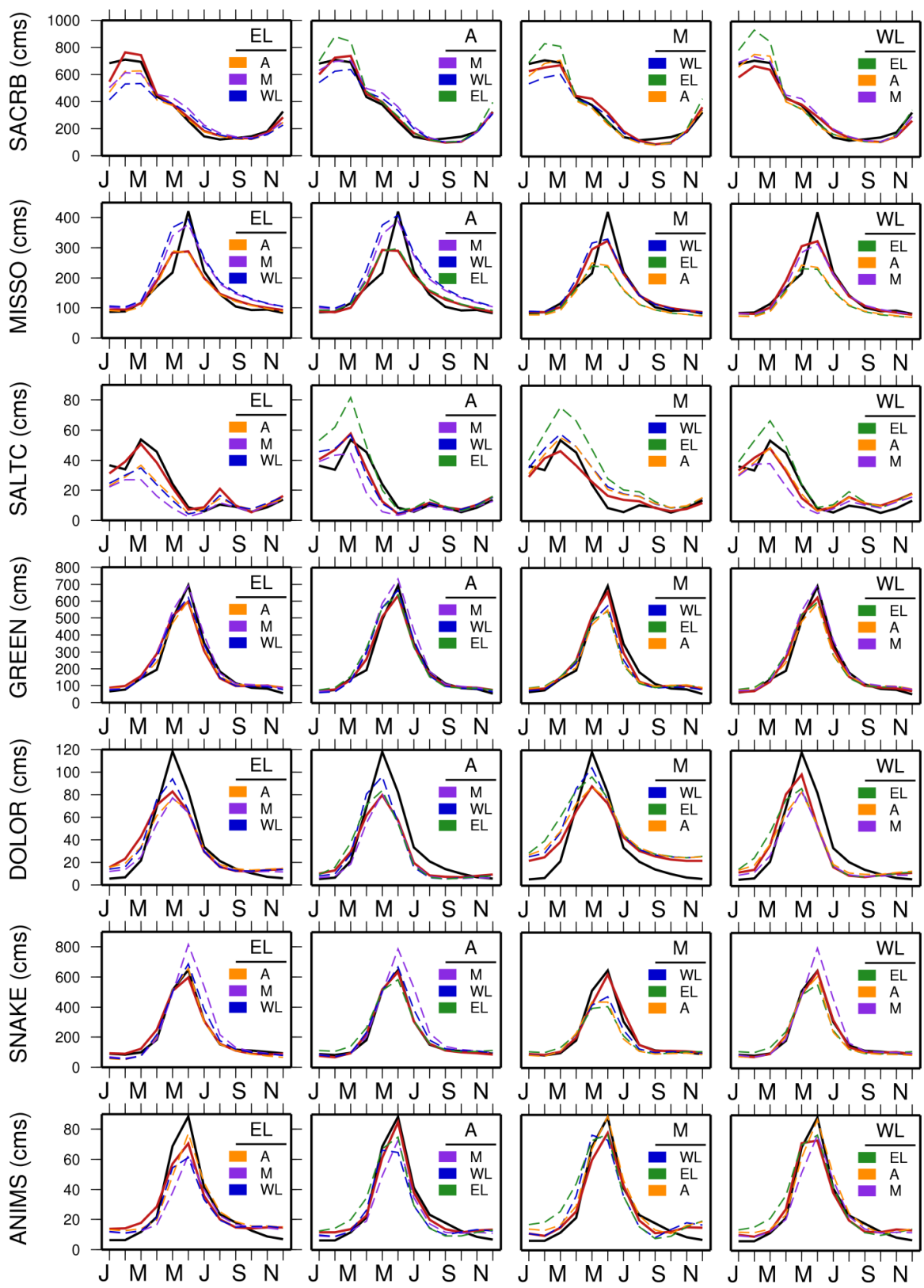


FIG 10. Change in mean annual precipitation (Prcp) vs. change in mean annual runoff (RO), computed between the calibration period and selected warm-dry years (circles) and cool-wet years (diamonds) in the validation period. Size of shapes represents the relative magnitude (absolute value) of corresponding change in mean annual temperature.

